# Depositional evolution of a progradational to aggradational, mixed-influenced deltaic succession: Jurassic Tofte and Ile formations, southern Halten Terrace, offshore Norway

Marijn van Cappelle[1,*], Rodmar Ravnås[2], Gary J. Hampson[1] & Howard D. Johnson[1]

[1]*Department of Earth Science and Engineering, Imperial College London, Royal School of Mines, Prince Consort Road, London, SW7 2BP, United Kingdom*

[2]*Norske Shell A/S, Tankvegen 1, Tananger, Norway*

**corresponding author: marijnvancappelle@gmail.com*

Hightlights:

- Core-based sedimentology of Jurassic deltaic strata from offshore Norway
- Facies analysis of tide-influenced deltaic and estuarine petroleum reservoirs
- Temporal development of deltaic deposits fed from multiple sediment sources
- Temporal development of tide-influenced deltaic deposits in a rift basin
- Synthesis of allocyclic and autocyclic processes on stratigraphic architecture

## Abstract

Predicting the hydrodynamics, morphology and evolution of ancient deltaic successions requires the evaluation of the three-dimensional depositional process regime based on sedimentary facies analysis. This has been applied to a core-based subsurface facies analysis of a mixed-energy, clastic coastal-deltaic succession in the Lower-to-Middle Jurassic of the Halten Terrace, offshore mid-Norway. Three genetically related successions with a total thickness of 100-300 m and a total duration of 12.5 Myr comprising eight facies associations record two initial progradational phases and a final aggradational phase. The progradational phases (I and II) consist of coarsening upward

successions that pass from prodelta and offshore mudstones (FA1), through delta front and mouth bar sandstones (FA2) and into erosionally based fluvial- (FA3) and marine-influenced (FA4) channel fills. The two progradational phases are interpreted as fluvial- and wave- dominated, tide-influenced deltas. The aggradational phase (III) consists of distributary channel fills (FA3 and FA4), tide-dominated channels (FA5), intertidal to subtidal heterolithic fine-grained sandstones (FA6) and coals (FA7). The aggradational phase displays more complex facies relationships and a wider range of environments, including (1) mixed tide- and fluvial-dominated, wave-influenced deltas, (2) non-deltaic shorelines (tidal channels, tidal flats and vegetated swamps), and (3) lower shoreface deposits (FA8). The progradational to aggradational evolution of this coastal succession is represented by an overall upward decrease in grain size, decrease in fluvial influence and increase in tidal influence. This evolution is attributed to an allogenic increase in the rate of accommodation space generation relative to sediment supply due to tectonic activity of the rift basin. In addition, during progradation, there was also an autogenic increase in sediment storage on the coastal plain, resulting in a gradual autoretreat of the depositional system. This is manifested in the subsequent aggradation of the system, when coarse-grained sandstones were trapped in proximal locations, while only finer grained sediment reached the coastline, where it was readily reworked by tidal and wave processes.

*Keywords: Ror Formation; Fangst Group; facies analysis; mixed energy delta; tide dominated; tide influenced*

## 1. Introduction

Coastal-deltaic depositional systems are commonly classified in terms of the relative interaction of wave, tide and fluvial processes (Galloway, 1975; Boyd et al., 1992). The facies characteristics of the three end members of this classification scheme can be defined with a reasonable level of confidence, supported by well described modern depositional systems (Penland et al., 1988; Dalrymple et al., 2003; Fanget et al., 2014). However, many ancient shallow-marine deposits display

evidence of mixed process regimes in which two or more processes were significant (i.e. they preserve mixed-energy depositional systems), which are more difficult to classify. Defining the relative interaction of processes in a precise way is challenging but also central to developing predictive process-oriented interpretations of coastal-deltaic reservoirs (Ainsworth et al., 2011).

The physical depositional processes controlling the character of clastic coastal deposits vary both spatially and temporally (Boyd et al., 1992; Ainsworth et al., 2011; Olariu, 2014), and these variations are reflected in vertical and lateral facies changes in paralic depositional systems (Hampson et al., 2011). A facies-based approach is applied herein to an evaluation of the Lower to Middle Jurassic Ror, Tofte and Ile formations of the southern Halten Terrace, offshore mid-Norway, which together constitute a net progradational to aggradational, mixed-influenced, coastal-deltaic succession, based on a particularly rich and high-quality subsurface database (Ravnås et al., 2014). The succession hosts significant oil and gas resources on the Halten Terrace (e.g. Alve, Åsgard, Heidrun, Kristin, Mikkel, Morvin, Njord, Norne, Skalv, Skuld and Urd fields; Harris, 1989; McIlroy, 2004; Morton et al., 2009; Norwegian Petroleum Directorate (NPD), 2016), but reservoir distribution and character are difficult to predict away from limited well penetrations in the southern Halten Terrace.

The overall distribution and structural setting of these formations are well known based on over 30 years of exploration evaluation and field development studies (Gjelberg et al., 1987; Blystad et al., 1995; Ravnås et al., 2014). However, detailed sedimentological analysis has been restricted to relatively small, hydrocarbon field-scale areas in the central and northern part of the Halten Terrace (Harris, 1989; McIlroy, 2004). The gross depositional setting of the Tofte and Ile formations is one of a progradational-to-aggradational clastic wedge that passes basinwards into marine mudstones (Gjelberg et al., 1987; Ravnås et al., 2014). Such clastic wedges may be (1) externally forced by temporal variations in the balance between relative sea-level and sediment supply (the "A/S ratio" *sensu* Muto and Steel, 1997) or, (2) record the internal response of the depositional system to steady external forcing (autoretreat *sensu* Muto and Steel, 1992; Muto 2001; Muto et al., 2007), or

by a combination of the two. The aims of this paper are: (1) to evaluate the spatial and temporal variations in the process regime (i.e. the relative degree of wave, tide and fluvial influence) of the Tofte and Ile formations; and (2) to develop a sedimentological and stratigraphic model that accounts for stratal architecture, grain-size partitioning (Strong et al., 2005; Bijkerk et al., 2016) and variations in depositional facies and process regime (Olariu, 2014), and (3) provide a framework for future prediction of sandstone reservoir distribution and character in the southern Halten Terrace.

## 2. Geological setting

The Halten Terrace is a N-S trending, 200 km long and 100 km wide, rhomboid shaped fault-bounded terrace offshore mid-Norway (Figure 1A,B). It is bounded by prominent, westward dipping Mesozoic extensional faults: (1) the Bremstein Fault to the east, (2) the Vingleia Fault to the southeast, (3) the Klakk Fault to the west, (4) a series of *en echelon* faults that make up the Revfallet Fault Complex to the north, and (5) the Kya Fault within the Halten Terrace (Figure 1B) (Blystad et al., 1995). These faults and the various bounding structural elements are the result of Mesozoic rifting between NW Europe and Greenland (Doré, 1991; Doré, 1992; Brekke et al., 2001).

The normal faults on the Halten Terrace ranges were intermittently active between the Permian and the Early Cretaceous, with temporal and spatial variations in the rate and amount of extensional displacement (Figure 2). The Bremstein Fault, which separates the Halten Terrace from the Trøndelag Platform (Figure 1B), and the Revfallet Fault Complex (outside of the study area in the north) were both active during Middle Jurassic (Garn Formation) to earliest Cretaceous (Spekk Formation) times (Corfield and Sharp, 2000; Richardson et al., 2005; Marsh et al., 2010; Wilson et al., 2013). In the northwestern part of the Halten Terrace (outside the study area), the Smørbukk and Trestakk faults were active between the Late Triassic (Åre Formation) and earliest Cretaceous (Spekk Formation). Upper Triassic to Lower Jurassic strata (Grey Beds, Åre, Tilje, Ror, Tofte and Ile formations; Figure 2), display subtle, fault-related thickness changes, whereas younger strata (Garn,

Melke and Spekk formations; Figure 2) exhibit more substantial thickness changes (Corfield and Sharp, 2000; Marsh et al., 2010).

The standard lithostratigraphic nomenclature of Dalland et al. (1988) has been adopted in this study (Figure 2). Triassic strata consist of continental red beds and evaporites (Grey Beds and Red Beds in Figure 2). Two distinct halite-bearing intervals have been recognized, which form a decollement interval for younger Mesozoic extensional faults (Jacobsen and Van Veen, 1984). During the Rhaetian to Hettangian, the Åre Formation was deposited as a series of coal-bearing alluvial and coastal plain deposits (Figure 2). Fluvial sandstone bodies in the upper part of the Åre Formation show evidence of tidal current action, indicating the onset of marine transgression, and are overlain by a series of retrogradationally stacked shoreface deposits (Thrana et al., 2014).

Three regressive-transgressive siliciclastic wedges define the Lower-Middle Jurassic strata of the Halten Terrace (Gjelberg et al., 1987). Ravnås et al. (2014) describe the regional distribution of the clastic wedges and the overall depositional process regimes, which were active during their deposition. The first (oldest) wedge (Pliensbachian to Toarcian) comprises the Tilje Formation (Figure 2) (Martinius et al., 2001; Martinius et al., 2005; Ichaso and Dalrymple, 2009; Ichaso and Dalrymple, 2014; Ichaso et al., 2016). The second wedge (Toarcian-Aalenian, 12.5 Myr) consists of the Ror, Tofte and Ile formations and has a thickness of 100-300 m (Harris, 1989; McIlroy, 2004; Ravnås et al., 2014). The third, and youngest (Bajocian-Bathonian) wedge comprises the Not and Garn formations (Figure 2) (Corfield et al., 2001; Messina et al., 2014). Increased rates of rifting commenced during deposition of the third wedge (Corfield and Sharp, 2000; Richardson et al., 2005; Marsh et al., 2010; Wilson et al., 2013). This resulted in widespread marine flooding followed by prolonged deposition of offshore shales of the Melke and Spekk formations (Dalland et al., 1988; Wilson et al., 2013).

## 3. Dataset and Methods

This study is based on data from 34 wells through the Ile, Tofte and Ror formations in the southern Halten Terrace (Figure 1C). Each well contains an extensive and consistent suite of wireline logs,

including gamma ray (GR), neutron porosity (NPHI) and bulk density (RHOB) logs, and there is high-quality core coverage from 19 wells (979 m of total core length). The cores were described on a 1:50 vertical scale (5 cm resolution). Facies analysis has been carried out based on lithology, grain-size and sorting, primary sedimentary structures, bioturbation index (BI, Taylor and Goldring, 1993) and trace fossil assemblages (MacEachern and Bann, 2008). Facies have been grouped into recurring facies associations. The facies associations were calibrated with their wireline log expression, in order to determine their diagnostic wireline log expression and their reservoir properties. The studied succession was subdivided into genetically related stratigraphic units in order to facilitate correlation and reservoir mapping (e.g. thickness, net sand and facies association proportions). Jurassic sediments in the footwall of the Vingleia and Bremstein fault zones have been buried deep (3.5-4.5 km), resulting in well compacted rocks with extremely well-preserved cores, which aids sedimentological observation. However, both seismic imaging and palynomorph preservation are poor, which limits their value in guiding high-resolution correlations within formations.

## 4. Facies analysis

A wide range of facies were identified and grouped into 8 facies associations. Figure 3 provides an overview of the facies and theirassociations in a graphical table form, Figure 4-6 show core photos that are representative of particular facies associations, and Figure 7 shows representative core logs for each facies association. The facies are on the 'element' or 'element set' scale of Vakarelov and Ainsworth (2013). The facies associations are on the 'element complex' scale and overall depositional environments discussed in section 5 are on the 'element complex set' and 'element complex assemblage' scale of Vakarelov and Ainsworth (2013).

### 4.1 FA1 Prodelta and offshore

#### 4.1.1 Description

FA1 is the mudstone-dominated part of coarsening upward facies successions of 10-50 m thick (Figure 3,7C,8). It consists of meters thick, dark, organic-rich and relatively homogeneous mudstones

(facies F1a), which pass gradationally upwards into mudstones containing centimetre-scale siltstone and very fine-grained sandstone layers and elongate, slightly asymmetrical ripples (facies F1b, Figure 4L). Rare asymmetrical ripples occur in the upper part of successions (facies F1d). Carbonaceous debris commonly lines individual laminae.

Bioturbation increases upwards in both intensity (from BI=0-3) and diversity. Trace fossils include *Planolites, Palaeophycus, Schaubcylindrichnus, Helminthopsis, Teichichnus, Thalassinoides, Ophiomorpha, Scolicia* and *Zoophycos* (Figure 4H-J). In some wells the BI is higher (BI=3-4) and there is an increase in trace fossil diversity, including the trace fossils *Scolicia, Palaeophycus* and *Cosmorhaphe* (facies F1c, Figure 4H-J). The sand content, bioturbation index (BI=2-5) and trace fossil diversity increase upwards, with the latter including *Planolites, Palaeophycus, Schaubcylindrichnus, Helminthopsis, Thalassinoides, Ophiomorpha, Scolicia* and *Zoophycos.* FA1 is gradationally overlain by FA2.

FA1 has a distinctive wireline log expression (wireline facies OS), most notably its high and upward decreasing GR profile (70-120 API). At the base of the Ror Formation, which is not cored, very high GR values of 100-150 API are present locally. FA1 is further characterized by high NPHI (10-30 %) and high RHOB (2.5-2.7 g/cm$^3$) values, which both decrease upward (e.g. in the Ror Formation in Figure 8).

### 4.1.2 Interpretation

The low-diversity trace fossil assemblage of facies F1a and F1b constitutes an impoverished distal *Cruziana* ichnofacies (MacEachern and Bann, 2008), which indicates deposition in a chemically stressed marine setting, possibly in a brackish prodelta environment where fresh and marine waters mixed (MacEachern and Bann, 2008). The mudstone-dominated lithology, low degree of bioturbation, high organic carbon content and abundant carbonaceous debris suggests sedimentation in a low-energy, stressed, dysoxic environment. The abundance of elongated, slight

asymmetrical ripples (F1b) and current ripples (F1d) may be indicative of offshore sediment transport by currents associated with fluvial discharge and/or storm-wave action (Arnott and Southard, 1990; Bohacs et al., 2014; Li et al., 2015). Those intervals with higher bioturbation indices and trace fossil diversities (facies F1c and F1d) reflect deposition in a less stressed and more open marine environment with lower deposition rates (MacEachern and Bann, 2008), probably in offshore areas lateral from the main sediment entry points along a deltaic coastline (Bohacs et al., 2014; Li et al., 2015).

## 4.2 FA2 Delta front and mouth bar

### 4.2.1 Description

FA2 gradually overlies FA1 although individual beds can have a sharp erosional base. FA2 consists of coarsening upward facies successions of very fine- to very coarse-grained sandstones with thicknesses of 3-30 m thick (Figure 3, 7C and 8). The basal part of the facies succession consists of 10-20 cm thick, very fine to fine-grained sandstone beds containing hummocky cross-stratification (HCS) (facies F2a, Figure 4E). This grades upward into very fine to medium-grained sandstones with current-ripple cross-lamination, with carbonaceous debris lining foreset laminae (facies F2b, Figure 4F). This coarsens upwards into medium- to coarse-grained, cross-bedded sandstones with set-thicknesses of 10-20 cm, often with mudstone clasts lining the toesets and foresets of cross-beds, and occasionally with mud drapes along their foresets (facies F2d, Figure 4G). The cross-bedded sandstones pass gradationally upwards into more poorly sorted, very coarse-grained sandstones with scattered granules (facies F2e). Individual beds fine upward, but the succession coarsens upwards overall.

The BI is low (0-2) and trace fossils include *Planolites, Palaeophycus, Skolithos, Rosselia* and escape traces. Locally the bioturbation is moderate in intensity (BI of 2-5) and more diverse,

including *Planolites, Palaeophycus, Ophiomorpha, Rosselia, Helminthopsis, Teichichnus, Schaubcylindrichnus* and *Thalassinoides* (facies F2c).

FA2 is characterized by high to upward-decreasing GR (20-70 API) and RHOB (2.1-2.5 g/cm$^3$) and low to upward-increasing NPHI (15-30 %) responses (e.g. in the Tofte Formation in Figure 8). The GR, RHOB and NPHI responses reflect the upward decrease in mudstone content and relative increase of porosity (wireline facies DF).

**4.2.2 Interpretation**

The coarsening-upward facies succession combined with abundant current ripple cross-lamination and dune-scale cross-bedding suggests upward shallowing in a subaqueous current-dominated setting (De Raaf et al., 1965; Wright, 1977; Elliott, 1978; Fielding et al., 2005a; Hampson et al., 2011). The coarse grain size and poor sorting within the highest energy facies is typical of deposition close to river mouths (Orton and Reading, 1993). The low intensity of bioturbation is consistent with high sedimentation rates in a delta front setting (MacEachern and Bann, 2008). The low diversity of trace fossil assemblages of the *Cruziana* and *Skolithos* ichnofacies also implies a stressed environment (MacEachern and Bann, 2008). This is consistent with a river mouth bar setting, where high sedimentation rates and fresh water inflow results in a stressed environment. Mud draped cross-stratification indicates that tidal currents influenced depositions (Boersma, 1969).

The presence of HCS in the lowest part of the succession indicates the influence of storm waves (Dott and Bourgeois, 1982; Duke, 1985; Keen et al., 2012). The absence of HCS in shallower and coarser grained parts of the succession may reflect the relatively coarse grain size, rather than a change in depositional processes (Dott and Bourgeois, 1982; Yoshida et al., 2007). The high degree of sorting in the coarser grained facies F2b-d is probably indicative of wave reworking (Yoshida et al., 2007; Hampson et al., 2011). This analysis suggests a mixed energy depositional setting, comprising a

fluvial- and/or wave-dominated and tide-influenced delta front environment (Fw*t* or Wf*t sensu* Ainsworth et al. 2011).

### 4.3 FA3 Fluvial channel

#### 4.3.1 Description

An erosional contact always separates FA3 from the underlying FA, most commonly FA1 or FA2. FA3 consists of sharp-based, 2-12 m thick, fining upward, medium- to very coarse-grained, poorly sorted sandstones, which locally contain granules and pebbles. A quartz pebble lag directly overlies the erosional basal contact. Subsequently, poorly sorted, cross-bedded pebbly sandstones (facies F3a, Figure 4B) pass upwards into moderately sorted cross-bedded sandstones. The cross beds have a set thickness of 10-30 cm (facies F3b, Figure 4A). Elsewhere, there are interbedded alternations of facies F3a and F3b separated by sharp boundaries. Homogenous, structureless mudstones (c. 0.5-1 m thick), with sharp tops and bases (facies F3c), are occasionally present and occur towards the top of the fining upward successions. Bioturbation is absent.

The wireline log values of FA3 are similar to those of FA2, but the logs show low and blocky to upward-increasing GR (20-50 API) and RHOB (2.1-2.5 g/cm3) responses and high and upward-decreasing NPHI (15-30 %) values. These responses correspond to the upward-fining trend of the facies succession (Figure 8). The thicker homogenous mudstones (facies F3c) are visible in the wireline logs (e.g. 50-150 API GR readings) but thinner layers are below vertical resolution (wireline facies CSS).

#### 4.3.2 Interpretation

The erosional base, poor sorting, upward decreasing grain size trend, primary sedimentary structures and absence of bioturbation are all consistent with fluvial channel deposition (Allen, 1965; Leeder, 1973). In places, the repeated interbedding of facies F3a and F3b may record multi-storey stacking of bars, consistent with deposition on rapidly migrating bars, possibly in braided rivers

(Miall, 1996; Hartley et al., 2016). The intervals of homogenous mudstones with sharp tops and bases which are interbedded with sandstones of this FA are interpreted to have been deposited in low-energy abandoned channels, because facies F3c occurs exclusively in the upper part of this upward fining facies succession (i.e. they overlie intervals of facies F1a and F1b). Evidence for tidal or wave influence is absent, suggesting that FA3 represents the deposits of purely fluvial channels (F *sensu* Ainsworth et al. 2011).

### 4.4 FA4 Marine-influenced fluvial channel

#### 4.4.1 Description

FA4 comprises fining upward successions of cross-stratified, moderate to very well sorted, fine- to very coarse-grained sandstones with a typical thickness of 2-10 m, but exceptionally up to 18 m. These overlie a sharp basal contact, which is often lined by a lag of quartz granules, pebbles and mud chips. The overlying cross-bedded sandstones with a set thickness of 10-30 cm contain mudstone laminae and mud chips in their toesets and along their foresets, which highlight cross-bed definition (facies F4a, Figure 4C). Farther upward, the deposits contain a similar suite of sedimentary facies but are moderately sorted (facies F4b, Figure 4D). These deposits are interbedded on a 5-50 cm scale with mud-draped, wavy-laminated, fine-grained sandstones (facies F4c) and heterolithic mudstones containing current-rippled sandstone lenses (facies F4e). Locally, homogenous, very well sorted, medium- to coarse-grained sandstones are present (facies F4d). These sandstones have a sharp base and show a slight upward decrease in sorting, which enables cross-bedding to be observed. Homogenous mudstones with a thickness of 1-5 cm are occasionally present in this facies.

Bioturbation in the sandstones (facies F4a-d) is generally low in intensity (BI=0-3) and trace fossils include O*phiomorpha, Skolithos, Palaeophycus* and C*ylindrichnus*. The heterolithic deposits of F4e contain *Planolites, Palaeophycus* and *Teichichnus*. The wireline log expression is indistinguishable from that of FA3 (wireline facies CSS), so the identification of FA4 depends on the availability of core (Figure 8).

#### 4.4.2 Interpretation

The sharp, erosional base and fining upward grain size trend of successions of FA4 suggests deposition in a channel. The poor sorting and coarse grain size of sandstones in the lower part of the succession indicates that texturally immature sediment was transported and deposited by strong unidirectional currents during times of high fluvial discharge (Dalrymple et al., 2015; Gugliotta et al., 2015; Gugliotta et al., 2016; Jablonski and Dalrymple, 2016). The presence of mud drapes and the heterolithic toesets of cross-beds is indicative of bedforms formed by tidal currents (Boersma, 1969; Terwindt, 1971; Van den Berg et al., 2007). The heterolithic mudstones and sandstones (facies F4c,e), which are interbedded with coarser grained sandstones, reflect tidal current deposition during periods of low fluvial discharge (Dalrymple et al., 2015; Gugliotta et al., 2016; Jablonski and Dalrymple, 2016). The homogenous mudstones (facies F4b and F4d) resemble fluid mudstones, indicating that wave action or tidal currents kept mud formed by salinity-induced mud flocculation in suspension (Ichaso and Dalrymple, 2009). The mature texture of well-sorted, medium- to coarse grained sandstones in facies F4d is attributed to sorting by waves, while the absence of HCS is attributed to the coarse grain size of available sediment (Yoshida et al., 2007). Cross-bedding in facies F4d may be due to dune migration in response to a combination of unidirectional fluvial, tidal and/or wave-generated longshore currents at the river mouth. The presence of the fluid mudstone deposits in this facies is not conclusive evidence for distinguishing between tide- and wave-generated currents (Ichaso and Dalrymple, 2009), but is consistent with deposition of facies F4d in an outer estuary mouth or in a river mouth subject to wave action. No evidence for sub-aerial exposure is present, so it is interpreted this FA was deposited in sub-tidal palaeo-water depths.

The presence of O*phiomorpha, Skolithos, Palaeophycus* and C*ylindrichnus*, which constitute the *Skolithos* ichnofacies, in the sandstone facies (F4a-F4d) signifies some marine influence, possibly brackish salinities, within a relatively unstable and rapidly shifting sandy substrate (MacEachern and Bann, 2008). The low diversity suites of *Planolites, Palaeophycus* and *Teichichnus* burrows

(*Teichichnus* ichnofacies) in heterolithic deposits (facies F4e) is consistent with deposition on bars with brackish salinities and intermittent sedimentation (e.g. as represented by the spreiten of *Teichichnus*) (Pemberton et al., 2009). In summary, FA4 represents deposition in tide-influenced, wave-influenced fluvial channels (Ft*w* succession *sensu* Ainsworth et al. 2011), and represents the transition between fluvial (FA3) and tidal (FA5) channel end-members.

### 4.5 FA5 Tidal channel

#### 4.5.1 Description

FA5 occurs laterally to FA3 and FA4, and is interbedded with FA6. It consists of 2-10 m thick, sharp-based, fining upward successions of heterolithic, very fine- to medium-grained sandstones. The base of successions of FA5 commonly comprises either a 1-5 cm-thick homogenous mudstone layer, or several thinner mudstone layers (facies F5a, Figure 5B,F). Bioturbation in these homogenous mudstones is low in intensity (BI=0-1) and diversity (*Palaeophycus* and *Planolites*). Overlying cross-bedded fine- to medium grained sandstones frequently contain 10-150 cm thick foresets that are lined with either mud chips or mud drapes (facies F5b, Figure 5B). These sandstones fine upward into very fine- to fine-grained sandstones with apparent bidirectional cross-lamination and current ripples, which also contain mud chips and mud drapes (facies F5c, Figure 5C). Bioturbation in the latter two facies is variable (BI 0-4), with trace fossils ranging from low diversity suites (*Palaeophycus* and *Planolites*) to more diverse suites that include *Lockeia, Gyrochorte, Ophiomorpha, Palaeophycus, Planolites, Cylindrichnus*, *Asterosoma* and escape traces. FA5 displays a variable wireline log expression. Where sandstone rich, FA5 has a similar response to FA3 and FA4 (wireline facies CSS), and where sandstone poor it appears similar to FA6 (wireline facies HFSS) (e.g. in the Ile Formation in Figure 8).

#### 4.5.2 Interpretation

The sharp, erosional base and fining upward heterolithic facies succession indicates deposition within a tidal channel (T or Tf *sensu* Ainsworth et al. 2011). This interpretation is supported by

abundant tidal indicators, most notably the fluid mudstones (Ichaso and Dalrymple, 2009), mud-draped cross-stratification (Boersma, 1969; Terwindt, 1971; Van den Berg et al., 2007) and apparent bidirectional current ripple cross-lamination (Reineck and Wunderlich, 1968). The fining upward heterolithic facies succession resembles those developed in tide-influenced point bars, which form inclined heterolithic strata (Reineck, 1958; Thomas et al., 1987; Choi et al., 2004). The large ranges in bioturbation intensity and trace fossil diversity indicate a wide range in environmental conditions. For example, the bispecific trace fossil suite of *Palaeophycus* and *Planolites* indicates chemical stress, most likely due to brackish salinities due to mixing of fresh river water and marine water (MacEachern and Bann, 2008). In contrast, the more diverse suites, which constitute the *Skolithos* and *Cruziana* ichnofacies indicate that these channels were connected to the sea, without the input of fresh water from fluvial sources (MacEachern and Bann, 2008). No evidence for sub-aerial exposure is present, so it is interpreted this FA was deposited in sub-tidal palaeo-water depths.

### 4.6 FA6 Tidal coastline

#### 4.6.1 Description

In general, FA6 gradationally overlies FA5 and has an erosional upper contact with FA5, but it is also less commonly interbedded with FA3 and FA4. At the top of the Ile Formation, FA6 is gradationally overlain by FA7. FA6 consists of 2-20 m thick successions heterolithic, very fine- to fine-grained sandstones containing two types of sedimentary structures. The first type (facies F6a) consists of 10-15 cm thick planar laminated, low angle cross-bedded, undulatory bedded and hummocky cross stratified, very fine- to fine grained sandstone beds (facies F6a, Figure 6A,B). The laminae within these beds are defined by sorting of grains of dark and light coloured mineralogies, and laminae are commonly paired (Figure 6B). The second type (facies F6b) consists of heterolithic, very fine- to fine grained, ripple scale cross-laminated sandstones, which appear planar over the width (c. 10 cm) of the core. The current ripple cross-lamination shows abundant apparent bidirectional palaeocurrent directions, which often have the same attitude and approach the angle of repose. The latter suggests

opposite palaeocurrent directions, although a component of different sections through 3D ripples cannot be completely excluded. Mud drapes are most common in the toesets and foresets of the cross-laminations (Figure 6A,C). The two dominant bedding styles (facies F6a and F6b) are interbedded on a decimetre-to-metre scale and may be overprinted by bioturbation of variable intensity (BI=0-5). In successions where facies F6a and F6b alternate, the beds of facies F6b are more intensely bioturbated than the adjacent beds of facies F6a. Beds that are destratified by the high intensity of bioturbation (BI=4-5) are classified separately as facies F6c. In all three facies, trace fossil diversity varies from sporadic occurrences of *Palaeophycus, Planolites* or *Skolithos* to more variable suites, including *Thalassinoides, Ophiomorpha, Cylindrichnus, Asterosoma, Rosselia, Teichichnus, Lockeia* and *Schaubcylindrichnus*. Facies F6a also contains escape traces. Generally, those beds with a lower bioturbation index also have a lower trace fossil diversity.

FA6 is characterized by a serrate GR log response (20-80 API), which reflects the centimetre-to metre-scale, heterolithic bedding style. NPHI values are generally low (5-15 %) and RHOB values are intermediate to high (2.3-2.7 g/cm$^3$) (wireline facies HFSS).

**4.6.2 Interpretation**

The mud-draped current ripple cross-lamination (facies F6b), with variable and possibly bidirectional palaeocurrent trends, resembles deposition from tidal currents (Reineck and Wunderlich, 1968). In contrast, the low-angle cross- bedded, very fine- to fine grained sandstone beds of facies F6a are interpreted as the expression in core of HCS (Scott, 1992), which resulted from storm wave action (Dott and Bourgeois, 1982; Duke, 1985; Keen et al., 2012). The paired laminae in these beds can be interpreted to reflect the daily inequality of semi-diurnal tides (Vakarelov et al., 2012; Wei et al., 2016). However, assuming that a single HCS bed is deposited by a single event (Figure 6B) implies that a single bed containing 30 paired laminae (Figure 6B) represents a storm with a duration of at least one month. More plausibly, the paired laminae can be attributed to sorting of different mineralogies during changing oscillation power of waves with alternating wave heights within a

wave group (Hamm et al., 1993). Some of the more planar laminated beds could also represent deposition by river floods caused by seasonal storms (Gugliotta et al., 2016), which simultaneously increase both the strength of unidirectional flows and the height, frequency and intensity of oscillatory waves ('storm flood'). Rapid deposition of these event beds is supported by the relatively low bioturbation intensity and the presence of escape traces. *Asterosoma* and *Schaubcylindrichnus* are indicative of relatively open marine conditions (MacEachern and Bann, 2008). This, and the close affinity with the channelised facies FA3, FA4 and especially FA5, which is usually gradationally overlain by FA6, suggests that deposition took place in subtidal to intertidal palaeo-water depths. This implies deposition in upper delta front to lower delta plain environments, within a tide-dominated, but wave- and fluvial-influenced, open coastline (Tw*f* or Tf*w sensu* Ainsworth et al. 2011). Neogene-to-modern tidal flat deposits are often rich in carbonaceous material (Van Straaten and Kuenen, 1957; Meor et al., 2013). However, large salt tolerant flora (e.g. mangroves) only evolved since the latest Cretaceous and flourished during the Neogene (Greb et al., 2006). Consequently, no abundant carbonaceous debris is expected in these Jurassic deposits, and neither is it observed. While such a mixed-energy coastline is common in the present-day, it is less commonly interpreted in the geological record (Johnson, 1975; Fan, 2012; Eide et al., 2016). The combination of HCS and heterolithic facies reworked by tidal currents has been observed in both modern linear coastlines with tidal flats (Yang et al., 2005; Fan, 2012) and their ancient equivalents (Basilici et al., 2012).

The trace fossil assemblages constitute the *Skolithos* and *Cruziana* ichnofacies (MacEachern and Bann, 2008), but their large variability in trace fossil intensity and diversity probably reflects variations in position with respect to the input of fresh water and sediment along the coastline (Li et al., 2011; Korus and Fielding, 2015; Ayranci and Dashtgard, 2015). In locations close to river mouths, brackish water and high sedimentation rates can result in impoverished trace fossil suites and low bioturbation intensity. In locations more distant from or updrift of river mouths, more fully marine

salinities and lower sedimentation rates resulted in more diverse and more intense bioturbation (MacEachern and Bann, 2008).

## 4.7 FA7 Coal mire

### 4.7.1 Description

FA7 gradationally overlies alternations of FA5 and FA6 and is only present in the top 20 m of the Ile Formation. FA7 consists of 20-50 cm thick cross-bedded (facies F7a) and current ripple cross-laminated (facies F7b), heterolithic (0-25 % mudstone) very fine- to fine-grained sandstones with rootlets and abundant disseminated carbonaceous debris. Capping these two facies, are 5-50 cm thick carbonaceous mudstone and coal beds (faciesF7c, Figure 5D,G). Bioturbation displays low intensity (BI=0-3) and diversity, and mainly consists of *Planolites, Cylindrichnus* and *Teichichnus.*

Wireline logs of facies F7a and F7b are similar to those of FA6. In contrast, the coals (facies F7c) are easily distinguished due to their low RHOB (<2 g/cm$^3$) and high NPHI (>45%) values (wireline facies CM).

### 4.7.2 Interpretation

The coals and underlying rootlet-penetrated sandstones indicate subaerial accumulation of peat in wetland conditions as histosols (Birkeland, 1999; Soil Survey Staff, 1999). The low-diversity trace fossil assemblage, which constitute impoverished *Cruziana* and *Skolithos* ichnofacies, and low bioturbation intensity in facies F7a and F7b supports a brackish, marginal marine setting (MacEachern and Bann, 2008). It is interpreted that the coals formed in a peat mire environment on the lower delta plain (Van Straaten and Kuenen, 1957).

## 4.8 FA8 Lower shoreface

### 4.8.1 Description

FA8 is only present in one well in the south of the study area, where it gradationally overlies mudstones of FA1. Towards the top of the Ile formation, FA8 is interbedded with coals of FA7. FA8 consists of successions of up to 20m thick of very fine- to fine-grained sandstone beds (10-30 cm), which are internally dominated by HCS, commonly overprinted by bioturbation of low intensity (BI=0-3) (facies F8a). The sandstone beds become increasingly amalgamated upwards, and intervening shales become correspondingly thinner and less abundant. Where bioturbation is more intense (BI=4-5), it obscures the HCS (facies F8b). Trace fossils include *Planolites, Palaeophyces, Schaubcylindrichnus, Thalassinoides, Teichichnus, Skolithos, Cylindrichnus, Lockeia*, *Ophiomorpha* and escape traces.

The wireline log expression of FA8 consists of multiple, stacked successions of high and upward-decreasing GR (30-70 API), NPHI (10-20 %) and RHOB (2.2-2.5 g/cm$^3$) values (wireline facies LSF).

#### 4.8.2 Interpretation

HCS indicates deposition under the influence of oscillatory waves between storm- and fair-weather wave-bases (Dott and Bourgeois, 1982; Duke, 1985; Keen et al., 2012). The high intensity of bioturbation and diverse trace fossil assemblage, which constitutes a mixed *Cruziana* and *Skolithos* ichnofacies, indicate deposition under fully marine conditions away from river-derived fresh water and sediment supply (MacEachern and Bann, 2008). FA8 therefore records wave-dominated deposition in the absence of tides or river influence (W *sensu* Ainsworth et al., 2011).

## 5. Vertical facies successions and lateral facies distributions

The facies analysis presented above provides the framework for interpreting vertical and lateral relationships between facies associations (Figure 8, 9). This allows interpretation of key stratal surfaces, notably marine flooding surfaces, and their lateral extent as determined from well log correlations (Figure 9). The succession comprises three genetically-related intervals, defined here in terms of depositional phases (from oldest to youngest): Phases I and II are progradational, and Phase

III is aggradational (Figure 8). The successions are correlated and mapped throughout the study area (Figure 9, 10), and a depositional model for each succession is presented (Figure 11).

## 5.1 Progradational Phase I

### 5.1.1 Description

This succession consists of mudstones of the Ror Formation and sandstones of the overlying Tofte Formation, and is bounded by two prominent marine flooding surfaces (Figure 8). The gross thickness of this mudstone-dominated succession varies between 200 m in the northwest and 100 m in the north, east and south (Figure 9, 10A). The log expression is characterized by a gradual upward decrease in GR, RHOB and NPHI values, which is bounded by two sharp upward increases in GR, RHOB and NPHI (Figure 8). The base of this succession is characterized by a thin (0-10 m) uncored interval with very high GR readings (>100 API; Figure 9), which is only present in the centre of the basin (Figure 10B). This is succeeded by a series of coarsening upward successions that comprise the following (from base to top): prodelta and offshore mudstones (FA1), mixed fluvial- and wave-dominated, tide-influenced delta front and mouth bar sandstones (FA2), and fluvial- (FA3) and marine-influenced fluvial channels (FA4). The coarsening upward successions average c. 20 m of thickness, with a range of 5 to 50 m (Figure 7A,C). Internally they are laterally variable, with individual coarsening upward successions only correlated over limited distances (c. 25-50 km), and not over the entire basin (c. 150 km) (Figure 9). The facies proportions are also variable, although FA1 and thin beds of FA2 are prominent in most wells. However, locally FA1 may occur in thinner intervals when the succession is dominated by sand-rich intervals of FA2, FA3 and FA4 (Figure 9). The net sandstone thickness, which reflects the thickness of FA2, FA3 and FA4, is greatest in the northwest (70 m) and decreases south-eastwards (10 m) before increasing in the east and southeast (50 m) (Figure 10C). The net channel-fill thickness (i.e. the combined thickness of FA3 and FA4) is also greatest in the northwest (40m), decreases south-eastwards to zero in the centre of the study area and increases again towards the east and southeast (10-40 m) (Figure 10D).

**5.1.2 Interpretation and depositional model**

The bounding surfaces of this succession represent abrupt increases in water depth from channelised sandstones (FA3, FA4) to marine mudstones (FA1), and are interpreted as maximum flooding surfaces based on their regional extent (Gjelberg et al., 1987; Ravnås et al., 2014). The thin interval of high GR values at the base of the succession is interpreted as a condensed section, reflecting very low deposition rates. The extent of the condensed section defines the basin-centre at this time (Figure 10B).

The coarse grain size (up to very coarse-grained and pebbly sandstone) of the coarsening upward successions (FA1, FA2, FA3 and FA4) suggests a high-energy and high-gradient fluvio-deltaic system. Similar sandstone textures in modern systems are often associated with braid deltas, which are dominated by high-discharge fluvial input (McPherson et al., 1987; Nemec and Postma, 1993; Orton and Reading, 1993). A braid delta interpretation is supported by sandstone distribution patterns (FA2, FA3 and FA5), which indicate a series of lobate protrusions from the opposite margins of the basin (Figure 10A, C, D). Evidence of storm wave reworking is provided by HCS (facies F2a) and by the well-sorted nature of the delta front and mouth bar sandstones (facies F2b, F2c and F2d). This can be compared to wave reworking in modern coarse-grained braid deltas, such as the Skeiðarársandur delta (Hine and Boothroyd, 1978), the Godavari delta (Nageswara Rao et al., 2005; Nageswara Rao et al., 2015) and, to a lesser extent, the more protected Burdekin delta (Fielding et al., 2005b; Fielding et al., 2005a; Fielding et al., 2006). Although tidal indicators are difficult to recognize in coarse-grained deposits and are therefore often not recognized (Dashtgard and Gingras, 2007), the presence of marine-reworked channels (FA4) implies that tides influenced some channels. Other potential modern analogues of such coarse grained deltas with tide-influence occur in bayhead deltas in fjords such as the Klimaklini and Honuthko (Syvitski and Farrow, 1983) and Bella Coola river deltas in Canada (Kostaschuk and McCann, 1983; Kostaschuk, 1985). However, descriptions of tide-influenced braid deltas in the geological record are sparse. The envisaged

depositional environment is a fluvial- and/or wave- dominated, tide-influenced braid delta (Wf*t* or Fw*t sensu* Ainsworth et al. 2011) (Figure 11A, B).

The successions are vertically stacked to define an overall progradational trend (Figure 8, 9). The northwest to southeast reduction in the total thickness, net sandstone thickness (FA2, FA3 and FA4) and proportion of channelised facies (FA3 and FA4) supports south-eastward delta progradation (Figure 10A, C, D), which downlapped onto the basin-centred condensed section (Gjelberg et al., 1987). The eastern margin of the basin displays an opposing trend, with a north-westwards reduction in net sandstone thickness (FA2, FA3 and FA4) and channelised facies proportions (FA3 and FA4) (Figure 10C, D). This indicates the north-westward progradation of either smaller delta lobes or the distal termination of a larger system to the southeast of the study area.

## 5.2 Progradational Phase II

### 5.2.1 Description

This succession is 30-100 m thick and consists of mudstones of the Ror Formation and overlying sandstones of the lower Ile Formation (Figure 8, 9, 10E). The base of the succession is marked by a sharp upward increase in GR, RHOB and NPHI values. The top is picked immediately above the lowermost channel-fill sandstone of the Ile Formation (FA3, FA4 or FA5) (Figure 8 and 9). This succession is laterally extensive across most of the study area, but is either absent or too thin (<2 m) to distinguish on certain horst blocks, particularly in the Njord Field (Figure 9B) and on the footwall of the Bremstein Fault Complex (Figure 9D, E, F). The significance of these thickness patterns is discussed later, in the context of younger strata (aggradational phase III; Figure 8).

This interval mainly comprises a single coarsening upward succession of prodelta and offshore mudstones (FA1), delta front and mouth bar sandstones (FA2) and channelised sandstones (FA3, FA4 and FA5) (Figure 8 and 9). In many locations there is an abrupt vertical change where erosionally-based channelised facies of FA3, FA4 and FA5 directly overlie marine mudstones of FA1 (e.g. well 6407/6-5; Figure 9). In this latter example, channel sandstones overlie an erosional surface lined by

quartz pebbles, while the preceding marine mudstones (FA1) also contain dispersed coarse sand grains and, occasionally, granules. The locations where the vertical succession is gradual (comprising FA2) form two broad north-south striking belts parallel to the basin margins (Figure 10F).

**5.2.2 Interpretation and depositional model**

The base of this succession is marked by an abrupt increase in water depth, which defines a regional flooding surface (Gjelberg et al., 1987; Ravnås et al., 2014). The overlying coarsening upward succession indicates the widespread, laterally-coalesced succession of fluvial- and wave- dominated, tide-influenced braid deltas (Wf*t*, Fw*t* or Ft*w sensu* Ainsworth et al. 2011) (Figure 10F). Hence, similar depositional environments characterised both Phases I and II (Figure 11A,B). However, the vertical and lateral stacking patterns of facies associations are different, most notably where channelised sandstones (FA3, FA4, FA5) directly overlie marine mudstones (FA1). These sharp-based, tide- and marine-influenced and partly channelised sandstones (FA3, FA4 and FA5) could represent the transgressive backfilling of an incised valley above a sequence boundary (Catuneanu, 2006; Dalrymple et al., 2006). However, the sharp-based sandstones form a laterally extensive sheet, which is inconsistent with elongate sand body geometries typical of valley-fills (Figure 9, 10F). In addition, the occurrence of coarse sand grains and granules beneath the erosion surface (in well 6407/6-5) suggests proximity to a contemporaneous coastline with coarse-grained fluvial sediment input. Hence, a forced regressive shoreline interpretation is proposed, in which prograding deltas followed a descending regressive trajectory (Posamentier and Morris, 2000; Helland-Hansen and Hampson, 2009; Prince and Burgess, 2013). In contrast, those locations comprising gradual coarsening upward facies successions (Figure 10H) record ascending regressive shoreline trajectories. Such successions occur in two north-south striking belts that lie east and west of the basin centre. It is interpreted that these two belts formed simultaneously as deltas from either side of the rift basin and prograded with ascending regressive shoreline trajectories during a time of increased A/S ratios. An explanation for increased creation of accommodation space could be

increased subsidence due to increased rift activity of the rift system which was intermittently active between the Triassic and Early Cretaceous (Ravnås and Steel, 1998). Modern analogues to this system, where fluvial-dominated deltas prograde into shallow water basins with a near-horizontal shoreline trajectory, include the modern Burdekin delta (Fielding et al., 2005a) and the Neogene and modern Volga delta (Kroonenberg et al., 1997; Overeem et al., 2003; Hinds et al., 2004; Kroonenberg et al., 2005). These examples contain sharp-based mouth bars and distributary channels that cut into offshore mudstones, similar to some of the Phase II successions.

## 5.3 Aggradational Phase III

### 5.3.1 Description

This succession corresponds to the middle and upper Ile Formation and has a thickness of c. 100 m in the west and thins gradually to c. 40 m in the east of the study area (Figure 8, 9, 10G). The base of this succession is picked at the top of the lowermost fluvial channel-fill sandstone (FA3, FA4 and FA5) in the Ile Formation. The top of the succession is defined by a sharp increase in GR, RHOB and NPHI values at the base of the Not Formation (Figure 2, 8). Internally, the GR, RHOB and NPHI values are low and show a slight upward increase (Figure 8, 9). The eastward thinning is gradual, except for locations on horst blocks, such as in the Njord Field (Figure 9B) and on the footwall of the Bremstein Fault Complex (Figure 9D, E, F). Where the Ile Formation is much thinner, progradational Phase II and aggradational Phase III cannot be distinguished from each other. Cores from these locations contain up to six firmground surfaces marked by the *Glossifungites* ichnofacies (MacEachern et al., 1992), which are not recognized elsewhere in thicker, more complete sections of the Ile Formation. These surfaces are also overlain by winnowed lags of granules and small pebbles (facies F6d, Figure 5A, E).

Phase III is dominated by vertical alternations of tidal channels (FA5) and tidal coastal deposits (FA6), with localised occurrences of cross-cutting channels (FA3 and FA4). Delta front successions (FA1, FA2) are absent, and the proportion of channel-fills (FA3, FA4 and FA5) decreases upwards. Channel-

fill sandstones are more abundant in the northeast and west (Figure 10G). Coal layers (FA7) occur towards the top of the succession, but only in the south (Figure 7B, D, 9B, E, F, 10F, H). Biostratigraphic data suggest that Phase III correlates with interbedded offshore mudstones (FA1), lower shoreface (FA8) and coals deposits (FA7) in the southwest (well 6406/11-1S in Figure 9A, F).

**5.3.2 Interpretation and depositional model**

The vertical stacking of abundant tide-influenced channel-fill sandstones (FA5) and tidal coastal plain deposits (FA6) throughout the succession implies aggradation of a lower delta plain with shallow subtidal to intertidal water depths. In this context, fluvial channel-fill sandstones lacking tidal influence (FA3) are interpreted as upper delta plain deposits that developed landward of the fluvial to tidal transition (Dalrymple et al., 1992; Dalrymple and Choi, 2007). The concentration of coals (FA7) in the upper part of the succession in the southern part of the study area reflects development of subaerial peat mire environments. Hence, water depth during Phase III deposition oscillated between shallow-subtidal to subaerial exposure, thereby recording a period of lower delta plain aggradation. The top of the succession is marked by an abrupt increase in water depth (Figure 2 and 8), which corresponds to a major, basin-wide flooding surface (Gjelberg et al., 1987; Ravnås et al., 2014).

During Phase III, two main types of shoreline were preserved: (1) non-deltaic wave-influenced tidal shorelines, and (2) mixed fluvial- and tide-dominated deltaic coastlines. Non-deltaic successions comprise alternating tidal channels (FA5) and tidal shorelines (FA6), which display high bioturbation intensity. In combination, these facies associations represent tide-dominated lower delta plains and associated coastlines, which were distant from active fluvio-deltaic sediment input points (Figure 11C,D) and subject to periodic storms and wave reworking (Yang et al., 2005; Basilici et al., 2012; Fan, 2012). In ancient and modern analogues of this type of non-deltaic coastline episodic HCS-bearing storm deposits are interbedded with tidal current ripples (Yang et al., 2005; Basilici et al., 2012). Only locally was there sufficient elevation and fresh ground-water to enable peat mires to

develop (FA7, Figure 10F). The envisaged depositional model was a tide-dominated and wave-influenced coastline (Tw *sensu* Ainsworth et al. 2011).

Deltaic successions are recognised where FA5 and FA6 display lower bioturbation intensity and diversity and where fluvial channels (FA3) and marine-influenced channels (FA4) are in close proximity. This would be consistent with relatively high sedimentation rates close to fresh water input points at river mouths (MacEachern and Bann, 2008; Li et al., 2011; Korus and Fielding, 2015; Ayranci and Dashtgard, 2015). The close association of fluvial- (FA3) and tide-influenced channels (FA4 and FA5) supports deposition in a mixed tide- and fluvial-dominated delta. Evidence for minor wave reworking in mouth bars (facies F4d) and tidal flats (facies F6a) indicates subordinate wave influence (Ft*w* or Tf*w sensu* Ainsworth et al. 2011) (Figure 11C,D). The Mahakam delta provides an analogue for a mixed energy, fluvial- and tide-influenced delta. The Mahakam delta plain comprises laterally adjacent active distributary fluvial channels and abandoned distributaries, which are effectively tide-dominated estuaries (Allen and Chambers, 1998). Active distributaries are filled with fine- to medium grained sand on much of the delta plain, and coarse-grained sand at the apex of the delta (Allen and Chambers, 1998; Salahuddin and Lambiase, 2013), which could be analogous to the grain size difference between FA3 and FA4. The abandoned distributary channels of the Mahakam contain a mix of mud and fine grained sand (Allen and Chambers, 1998; Salahuddin and Lambiase, 2013), which compares favourably to the heterolithic very fine- to fine grained tidal channels of FA5. The higher proportion of finer grained tide-dominated channels in the modern Mahakam delta plain is also comparable to that seen in the Phase III succession (Figure 9). Ancient analogues can be found in the Cretaceous Sego Sandstone, USA (Willis and Gabel, 2001; Willis and Gabel, 2003; Legler et al., 2014; Van Cappelle et al., 2016), the Jurassic Neill Klinter Group, Greenland (Dam and Surlyk, 1998; Ahokas et al., 2014; Eide et al., 2016) and the Jurassic Lajas Formation, Argentina (McIlroy et al., 2005; Gugliotta et al., 2015; Rossi and Steel, 2016). Each of these three examples contains similar aggradational successions to those documented during Phase III deposition, containing (1) relatively coarse-grained fluvial channel-fill sandstones (cf. FA3, FA4), (2) relatively fine-grained and

heterolithic tidal channel-fill sandstones (cf. FA5), and (3) wave-reworked mouth bar and delta front sandstones. The Neill Klinter Group also contains heterolithic tidal flat deposits (cf. FA6). Fluvial channel-fill sandstones in the Lajas Formation and Neill Klinter Group are pebbly and coarse-grained, as are those in the Ile Formation.

In aggradational Phase III, a higher proportion of coarse-grained channel-fill sandstones (FA3, FA4 and FA5) are present in the east, north and west, which correlate to offshore mudstones (FA1), shoreface sandstones (FA8) and coal mire deposits (FA7) to the southwest in well 6406/11-1S (Figure 10F, H). In the context of the regional setting (Figure 1A), it is interpreted that sediment input was transverse to the rift axis, both from the west and east, and along the rift axis from the north. The occurrence of offshore (FA1) and shoreface (FA8) deposits to the south can be explained by three possible scenarios: (1) a change in depositional process from tide-dominated to wave-dominated, due to progradation along the rift-axis, which widened to the south (Fig. 1A) (Legler et al., 2014; Olariu, 2014); (2) wave-dominated deposition was contemporaneous with the tide-dominated deposition along the depositional strike of the shoreline outside of the embayment; and (3) sedimentation could have been locally sourced from a neighbouring horst block or uplifted footwall (Ravnås and Steel, 1998).

The restricted occurrence of coals (FA8) in the south can be explained in two ways: (1) a coal-bearing lower delta plain environment was located in the south, with a coeval, non-coal-bearing upper delta plain in the north; and (2) coals only developed locally on slowly subsiding or uplifted horst blocks and footwall blocks associated with faults that were active during Ile deposition.

The reduced thickness of Phase II and Phase III successions (Figure 8) on the Njord Field horst block (Figure 9B) and in the footwall of the Bremstein Fault Complex (Figure 9D, E, F) confirms active faulting during deposition of Phases II and III. This is supported by evidence of erosion and winnowing by wave and/or tidal action in these areas, which resulted in the localised occurrence of firmgrounds and lags within the Ile Formation. Subsequently, uplift of the footwall of the Bremstein

Fault Complex resulted in the erosion and thinning of Ile Formation in the Draugen Field (Figure 9E, F) (Goesten and Nelson, 1992; Provan, 1992).

## 6. Stratigraphic models for temporal evolution of the "Tofte and Ile deltas"

A stratigraphic model is outlined below to account for the temporal and spatial changes in the grain size characteristics and depositional process regime during the deposition of Phases I to III. The model considers the observed stratal architectures, grain size characteristics and facies patterns within the context of the sediment routing systems, from source area to depositional sink (Figure 12A).

### 6.1 Catchment and hinterland

Transverse catchments feeding rift basins are usually numerous, but relatively small, because they are developed in the footwall of faults bounding rotated intra-basinal or basin-marginal blocks (Leeder and Gawthorpe, 1987; Ravnås and Steel, 1998; Ravnås et al., 2000). However, the abundance of coarse grained, extra-basinal sediment, which cannot be derived from reworking the finer grained, underlying successions, precludes local, intra-basinal source areas. It has been proposed that some of the sediment at the Halten Terrace was derived from Greenland (Morton et al., 2009). However, the presence of a palaeo-high between the Baltic Shield and Greenland (Doré, 1992; Nøttvedt et al., 2008; Eide et al., 2016) precludes a source of sediment as far Greenland (Figure 12A). The Halten Terrace may have formed part of a fault-bounded, south-facing embayment with major sediment sources to the west, east and along the axis of the rift to the north, and a sink in the rift-axis to the south (Ziegler, 1988; Doré, 1992). This is consistent with regional reconstructions (Gjelberg et al., 1987; Ravnås et al., 2014), in which the Jurassic strata of the Halten Terrace were deposited in the same seaway as age equivalent strata on East Greenland (Surlyk, 1990; Alsgaard et al., 2003; Vosgerau et al., 2004; Eide et al., 2016). Relatively short source catchments in the Baltic Shield were present east of the Halten Terrace during the Cretaceous (Martinsen et al., 2005; Elliott et al., 2012; Elliott et al., 2015; Sømme et al., 2013), and it has been

assumed that a similar catchment was present during the Jurassic. The northern limit of the catchment is poorly constrained.

### 6.2 Change from progradation (Phases I and II) to aggradation (Phase III) to transgression (Not Formation)

The change from net progradation (Phases I and II) to net aggradation (Phase III), followed by regional transgression (basal Not Formation), can be explained by a combination of two possible mechanisms. In the first model, the stratal architecture may record a cycle of relative sea-level and/or sediment supply change (i.e. decreasing and then increasing A/S ratio). In this interpretation, (1) net progradation is due to sediment supply being greater than the rate of accommodation creation (A/S < 1), (2) aggradation reflects sediment supply being in balance with the rate of accommodation creation (A/S = 1), and (3) transgression reflects accommodation creation outpacing sediment supply (A/S > 1). In rift basins, such conditions occur during inter-rift periods of tectonic quiescence when subsidence rates are reduced while sediment supply remains constant (Ravnås and Steel, 1998; Ravnås et al., 2000; Ravnås et al., 2014).

In the second model, the stratal architecture may represent autoretreat (Muto and Steel, 1992; Muto, 2001; Muto et al., 2007) of the deltas under conditions of constant sediment supply and a constant rate of accommodation creation (i.e. constant A/S ratio). Such boundary conditions may occur in rift settings, such as the Halten Terrace, during times of tectonic quiescence when subsidence rates and sediment supply are constant (Muto and Steel, 1992). Under such conditions, deltas may prograde initially across the antecedent basin-floor topography. However, the total surface area of deposition on the delta plain increases as progradation continues, and progressively more of the supplied sediment is trapped within the expanding delta plain. Therefore the sediment supply to the shoreline progressively decreases, causing a reduced shoreline progradation rate and eventual retrogradation without any external forcing.

The models are not mutually exclusive, so a combination of both models may have influenced the study area. Initially simultaneous delta progradation from all the sediment delivery pathways suggests that an allogenic forcing mechanism drove the progradation. Delta progradation and progressively higher rates of sediment accumulation on the delta plain may have driven autogenic aggradation and autoretreat (Muto and Steel, 1992; Muto and Steel, 2001). According to Muto et al. (2007) the first order estimation for the timescale of onset of autogenic events equates to:

$$\tau = \alpha \frac{S}{|A|^2} \quad \text{(Eq. 1)}$$

In which τ is the timescale for onset of autogenic events, α is the slope of the alluvial plain, S is the rate of sediment supply, and A is the rate of accommodation space creation. The architecture and dimensions of the major axial routing system during progradation (Phases II) and aggradational (Phase III) had the following cross-sectional geometry (Figure 12B) and timescales: (1) length scale (250-500 km), (2) thickness (100-150 m), and (3) assumed slope of the coastal plain (0.01-0.001°) (Miall, 1991; Robinson and Slingerland, 1998), and (4) a duration of 5-10 Ma. Based on this depositional framework, the time scale for autoretreat of the axial system is estimated at 0.15-9 Myr. This is shorter in duration than the observed maximum duration for progradation-to aggradation of Phases II and III of 5-10 Myr (Ror and Ile formations, Figure 2). Therefore the geometry and timing of the system are in agreement with autoretreat as a possible mechanism to explain the observed progradation and aggradation. The abrupt flooding at the top of aggradational Phase III is explained by renewed rift activity (Ravnås and Steel, 1998; Ravnås et al., 2000; Ravnås et al., 2014) causing increased subsidence, which rapidly terminated autoretreat (*cf.* Fig. 6A of Muto et al., 2007).

### 6.3 Sediment dispersal and mass balance considerations

For sediment routing systems with a closed sediment budget, and a uniform proportion of input grain sizes, the theory of mass balance predicts that downsystem transitions in grain size and associated facies belts occur at fixed locations along a length scale normalised to deposited

sediment mass (Strong et al., 2005). In either of the allogenic and autogenic forced models outlined above, progradation followed by aggradation implies that the grain size transitions reflect upstream retreat of the sediment routing system over time, as a progressively greater proportion of sediment mass is stored on the delta plain (Muto and Steel, 1992). By implication, mass balance consideration for progradational- to aggradational systems implies that the coarsest grain sizes in lower delta plain and delta front deposits will be encountered during initial progradation, when pebbly, coarse sand was transported to the coastline where it was deposited in mouths bars (FA2) and distributary channels (FA3,FA4). During this period, fine-grained sand may have been bypassed to the basin floor, as is common in coarse-grained deltas (Walker, 1966; Hampson, 1997; Rohais et al., 2008; Backert et al., 2010), transported alongshore out of the study area (Hampson et al., 2014) or the input sediment supply may have lacked this grain size fraction (Michael et al., 2013). During subsequent delta plain aggradation, pebbly, coarse sand could have been stored in fluvial channels (FA3) on the upper delta plain, with only very fine-to-medium sand reaching the lower delta plain, where it was deposited in tidal flats and channels (FA5, FA6; Fig. 12B,C).

### 6.4 Link to depositional process regime

The depositional process regime of siliciclastic coastlines is influenced by several, partly linked factors such as grain size, river gradient and length (McPherson et al., 1987; Orton and Reading, 1993; Dashtgard and Gingras, 2007), shelf width and changes in shoreline morphology during regressions and transgressions (Boyd et al., 1992; Ainsworth et al., 2011; Olariu, 2014). Therefore, the change from progradation in Phase II to aggradation in Phase III and the related decrease in sandstone grain size affects the preserved record of depositional process regimes. It is widely accepted that depositional systems become more tide-dominated during transgressions as the coastline rugosity increases and tidal currents are amplified in newly formed coastal embayments and drowned fluvial valleys (Boyd et al., 1992; Dalrymple, 2006; Yoshida et al., 2007). Also, coarse grained coastal deposits are more likely to be dominated by fluvial processes due to the proximity of these coastlines to the hinterland and the related more rapid response to changes in sediment

supply from the hinterland (Hine and Boothroyd, 1978; Kostaschuk and McCann, 1983; Syvitski and Farrow, 1983; Kostaschuk, 1985; McPherson et al., 1987; Orton and Reading, 1993; Fielding et al., 2005b; Fielding et al., 2006). In addition, recognition of tidal process in coarse grained deposits is problematic (Dashtgard and Gingras, 2007). Consequently, the change in depositional process from fluvial and wave dominated in progradational Phase I and Phase II to more tide dominated processes in aggradational Phase III may reflect a combination of (1) change in coastal behaviour (Olariu, 2014), and (2) the available sediment texture (Dashtgard and Gingras, 2007).

## 7. Conclusions

- The Early to Middle Jurassic Ror, Tofte and Ile formations of the Halten Terrace, offshore mid-Norway preserves three genetically-related phases of clastic coastal-deltaic deposition, with distinct mixed-influenced process regimes. The older Phases I and II are progradational, and the younger Phase III is aggradational.
- The deposits of Phase I (100-200 m thick) represent a series of progradationally-stacked, mixed fluvial- and/or wave- dominated, tide-influenced braid deltas. The main delta system prograded southeastward, transverse to the rift axis. A series of minor deltas prograded westward from the opposite eastern margin of the basin.
- The deposits of Phase II (30-70 m thick) represent a similar depositional environment to those of Phase I, but record only a single period of progradation. Commonly the channel fill deposits erosionally overlie marine mudstones, indicating that part of the progradation occurred with a descending regressive shoreline trajectory. In contrast, gradational coarsening upward successions were deposited during a period of ascending regressive shoreline trajectories.
- The deposits of Phase III (40-100 m thick) are the result of aggradational stacking of (1) mixed tide- and fluvial-dominated (wave-influenced) delta deposits, and (2) non-deltaic tide-dominated, wave-influenced coastline deposits. These two environments were contemporaneous and record a spatial change in depositional process regime.

- The decrease in grain size, decrease in fluvial influence and increase in tide influence from progradational Phase II to aggradational Phase III is interpreted to be the result of a combination of quiescence in rift activity and autogenic retreat of the delta front. Initially, reduction in rift activity caused a decreasing A/S ratio. This resulted in delta progradation from multiple source areas. During progradation from the W, NE and E, an increasing proportion of the available sediment was stored on the lower delta plain, causing a decrease in progradation rate followed by delta aggradation (i.e. autoretreat). Eventually renewed tectonic activity resulted in abrupt flooding at the top of aggradational Phase III. Assuming that the proportion of different grain-sizes in the sediment supply were time invariant, and a that an increasing proportion of the sediment budget was deposited on the delta topset, then mass balance considerations predict a decrease in grain size during delta topset aggradation, as observed in the change from Phase II to Phase III. The change from progradation to aggradation, and the related change in available grain size, may have enhanced the preservation signature of tidal processes.

## Acknowledgement

Funding of the study and approval for publication by Shell International and Norske Shell are gratefully acknowledged. The Department of Earth Science and Engineering of Imperial College is thanked for the award of a Janet Watson PhD scholarship. We thank Kyungsik Choi, Alex Coleman, Daniel Collins, Caroline Hern, Chris Jackson and Ru Smith for discussions. Aitor Ichaso, Christian Haug Eide and an anonymous reviewer are thanked for their constructive reviews.

## References

Ahokas, J.M., Nystuen, J.P., Martinius, A.W., 2014. Depositional dynamics and sequence development in a tidally influenced marginal marine basin: Early Jurassic Neill Klinter Group, Jameson Land Basin, East Greenland, in: Martinius, A.W., Ravnås, R., Howell, J.A., Steel, R.J., Wonham, J.P. (Eds.), From Depositional Systems to Sedimentary Successions on the Norwegian Continental Margin, IAS Spec. Publ. 46, pp. 291-338.

Ainsworth, R.B., Vakarelov, B.K., Nanson, R.A., 2011. Dynamic spatial and temporal prediction of changes in depositional processes on clastic shorelines: Toward improved subsurface uncertainty reduction and management. AAPG Bull. 95, 267-297.

Allen, G.P., Chambers, J.L.C., 1998. Sedimentation in the Modern and Miocene Mahakam Delta. Indonesian Petroleum Association, Jakarta.

Allen, J.R.L., 1965. Fining-upwards cycles in alluvial successions. Geol. J. 4, 229-246.

Alsgaard, P.C., Felt, V.L., Vosgerau, H., Surlyk, F., 2003. The Jurassic of Kuhn Ø, North-East Greenland. Geol. Surv. Den. Greenl. 1, 865-892.

Arnott, R.W., Southard, J.B., 1990. Exploratory flow-duct experiments on combined-flow bed configurations, and some implications for interpreting storm-event stratification. J. Sed. Res. 60, 211-219.

Ayranci, K., Dashtgard, S.E., 2015. Asymmetrical deltas below wave base: Insights from the Fraser River Delta, Canada. Sedimentology 63, 761-779.

Backert, N., Ford, M., Malartre, F., 2010. Architecture and sedimentology of the Kerinitis Gilbert-type fan delta, Corinth Rift, Greece. Sedimentology 57, 543-586.

Basilici, G., Vieira de Luca, P.H., Paiva Oliveira, E., 2012. A depositional model for a wave-dominated open-coast tidal flat, based on analyses of the Cambrian-Ordovician Lagarto and Palmares formations, north-eastern Brazil. Sedimentology 59, 1613-1639.

Bijkerk, J.F., Eggenhuisen, J.T., Kane, I.A., Meijer, N., Waters, C.N., Wignall, P.B., McCaffrey, W.D., 2016. Fluvio-marine sediment partitioning as a function of basin water depth. J. Sed. Res. 86, 217-235.

Birkeland, P.W., 1999. Soils and Geomorphology. Oxford University Press, New York.

Blystad, P., Brekke, H., Færseth, R.B., Larsen, B.T., Skogseid, J., Tørudbakken, B., 1995. Structural elements of the Norwegian continental shelf Part II: The Norwegian Sea Region. NPD Bull. 8, 2-45.

Boersma, J.R., 1969. Internal structure of some tidal mega-ripples on a shoal in the Westerschelde Estuary, the Netherlands, report of a preliminary investigation. Geol. Mijnbouw 48, 409-414.

Bohacs, K.M., Lazar, O.R., Demko, T.M., 2014. Parasequence types in shelfal mudstone strata—Quantitative observations of lithofacies and stacking patterns, and conceptual link to modern depositional regimes. Geology 42, 131-134.

Boyd, R., Dalrymple, R., Zaitlin, B.A., 1992. Classification of clastic coastal depositional environments. Sediment. Geol. 80, 139-150.

Brekke, H., Sjulstad, H.I., Magnus, C., Williams, R.W., 2001. Sedimentary environments offshore norway — an overview, in: Martinsen, O.J., Dreyer, T. (Eds.), Sedimentary Environments Offshore Norway — Palaeozoic to Recent, NPF Spec. Publ. 10, pp. 7-37.

Catuneanu, O., 2006. Principles of Sequence Stratigraphy. Elsevier, Amsterdam, Oxford.

Choi, K.S., Dalrymple, R.W., Chun, S.S., Kim, S., 2004. Sedimentology of Modern, Inclined Heterolithic Stratification (IHS) in the Macrotidal Han River Delta, Korea. J. Sed. Res. 74, 677-689.

Corfield, S., Sharp, I.R., 2000. Structural style and stratigraphic architecture of fault propagation folding in extensional settings: a seismic example from the Smørbukk area, Halten Terrace, Mid-Norway. Basin Res. 12, 329-341.

Corfield, S., Sharp, I., Häger, K., Dreyer, T., Underhill, J., 2001. An integrated study of the Garn and Melke formations (Middle to Upper Jurassic) of the Smørbukk area, Halten Terrace, mid-Norway, in: Martinsen, O.J., Dreyer, T. (Eds.), Sedimentary Environments Offshore Norway — Palaeozoic to Recent, NPF Spec. Publ. 10, pp. 199-210.

Dalland, A., Worsley, D., Ofstad, K., 1988. A lithostratigraphic scheme for the Mesozoic and Cenozoic succession offshore mid- and northern Norway. NPD Bull. 4, 1-65.

Dalrymple, R.W., Kurcinka, C.E., Jablonski, B.V.J., Ichaso, A.A., Mackay, D.A., 2015. Deciphering the relative importance of fluvial and tidal processes in the fluvial-marine transition, in: Ashworth, P.J., Best, J.L., Parsons, D.R. (Eds.), Fluvial-Tidal Sedimentology, Dev. Sed. 68, pp. 3-45.

Dalrymple, R.W., 2006. Incised Valleys in Time and Space: An Introduction to the Volume and an Examination of the Controls on Valleys Formation and Filling, in: Dalrymple, R.W., Leckie, D.A., Tillman, R.W. (Eds.), Incised Valleys in Time and Space, SEPM Spec. Publ. 85, pp. 5-12.

Dalrymple, R.W., Baker, E.K., Harris, P.T., Hughes, M.G., 2003. Sedimentology and stratigraphy of a tide-dominated foreland-basin delta (Fly River, Papua New Guinea), in: Hasan Sidi, F., Numedal, D., Imbert, P., Darman, H., Posamentier, H. (Eds.), Tropical Deltas of Southeast Asia- Sedimentology, Stratigraphy, and Petroleum Geology, SEPM Spec. Publ. 76, pp. 147-173.

Dalrymple, R.W., Choi, K., 2007. Morphologic and facies trends through the fluvial–marine transition in tide-dominated depositional systems: A schematic framework for environmental and sequence-stratigraphic interpretation. Earth-Sci. Rev. 81, 135-174.

Dalrymple, R.W., Leckie, D.A., Tillman, R.W., 2006. Incised Valleys in Time and Space, SEPM Spec. Publ. 85 ed.

Dalrymple, R.W., Zaitlin, B.A., Boyd, R., 1992. Estuarine facies models; conceptual basis and stratigraphic implications. J. Sed. Res. 62, 1130-1146.

Dam, G., Surlyk, F., 1998. Stratigraphy of the Neill Klinter Group; a Lower - lower Middle Jurassic tidal embayment succession, Jameson Land, East Greenland. Geol. Surv. Den. Greenl. 175, 1-80.

Dashtgard, S.E., Gingras, M.K., 2007. Tidal Controls on the Morphology and Sedimentology of Gravel-Dominated Deltas and Beaches: Examples from the Megatidal Bay of Fundy, Canada. J. Sed. Res. 77, 1063-1077.

De Raaf, J.F.M., Reading, H.G., Walker, R.G., 1965. Cyclic sedimentation in the lower Westphalian of no Devon, England. Sedimentology 4, 1-52.

Doré, A.G., 1992. Synoptic palaeogeography of the Northeast Atlantic Seaway: late Permian to Cretaceous, in: Parnell, J. (Ed.), Basins on the Atlantic Seabord: Petroleum Geology, Sedimentology and Basin Evolution, Geol. Soc. Spec. Publ. 62, pp. 421-446.

Doré, A.G., 1991. The structural foundation and evolution of Mesozoic seaways between Europe and the Arctic. Palaeogeogr. , Palaeoclimatol. , Palaeoecol. 87, 441-492.

Dott, R.H., Bourgeois, J., 1982. Hummocky stratification: Significance of its variable bedding sequences. Geol. Soc. Am. Bull. 93, 663-680.

Duke, W.L., 1985. Hummocky cross-stratification, tropical hurricanes, and intense winter storms. Sedimentology 32, 167-194.

Eide, C.H., Howell, J.A., Buckley, S.J., Martinius, A.W., Oftedal, B.T., Henstra, G.A., 2016. Facies model for a coarse-grained, tide-influenced delta: Gule Horn Formation (Early Jurassic), Jameson Land, Greenland. Sedimentology .

Elliott, F., 1978. Deltas, in: Reading, H.G. (Ed.), Sedimentary Environments and Facies, pp. 113-154.

Elliott, G.M., Jackson, C.A.L., Gawthorpe, R.L., Wilson, P., Sharp, I.R., Michelsen, L., 2015. Late syn-rift evolution of the Vingleia Fault Complex, Halten Terrace, offshore Mid-Norway; a test of rift basin tectono-stratigraphic models. Basin Res.

Elliott, G.M., Wilson, P., Jackson, C.A.L., Gawthorpe, R.L., Michelsen, L., Sharp, I.R., 2012. The linkage between fault throw and footwall scarp erosion patterns: an example from the Bremstein Fault Complex, offshore Mid-Norway. Basin Res. 24, 180-197.

Engkilde, M., Surlyk, F., 2003. Shallow marine syn-rift sedimentation: Middle Jurassic Pelion Formation, Jameson Land, East Greenland. Geol. Surv. Den. Greenl. 1, 813-863.

Fan, D., 2012. Open-Coast Tidal Flats, in: Davis, R.A., Dalrymple, R.W. (Eds.), Principles of Tidal Sedimentology, pp. 187-229.

Fanget, A., Berné, S., Jouet, G., Bassetti, M., Dennielou, B., Maillet, G.M., Tondut, M., 2014. Impact of relative sea level and rapid climate changes on the architecture and lithofacies of the Holocene Rhone subaqueous delta (Western Mediterranean Sea). Sediment. Geol. 305, 35-53.

Fielding, C.R., Trueman, J.D., Alexander, J., 2006. Holocene Depositional History of the Burdekin River Delta of Northeastern Australia: A Model for a Low-Accommodation, Highstand Delta. J. Sed. Res. 76, 411-428.

Fielding, C.R., Trueman, J.D., Alexander, J., 2005a. Sharp-Based, Flood-Dominated Mouth Bar Sands from the Burdekin River Delta of Northeastern Australia: Extending the Spectrum of Mouth-Bar Facies, Geometry, and Stacking Patterns. J. Sed. Res. 75, 55-66.

Fielding, C.R., Trueman, J., Alexander, J., 2005b. Sedimentology of the modern and Holocene Burdekin river delta of North Queensland, Autralia- Controlled by river output, not waves and tides, in: Giosan, L., Bhattacharya, J.P. (Eds.), River Deltas-Concepts, Models, and Examples, SEPM Spec. Publ. 83, pp. 467-496.

Galloway, W.E., 1975. Process Framework for Describing the Morphologic and Stratigraphic Evolution of Deltaic Depositional Systems, in: Broussard, M.L. (Ed.), Deltas: Models for Exploration, pp. 87-98.

Gjelberg, J., Dreyer, T., Høie, A., Tjelland, T., Lilleng, T., 1987. Late Triassic to Mid-Jurassic sandbody development on the Barents and Mid-Norwegian shelf, in: Brooks, J., Glennie, K.W. (Eds.), Petroleum Geology of North West Europe, London, pp. 1105-1129.

Goesten, M.J.B.G., Nelson, P.H., 1992. Draugen Field - Norway, North Sea Basin, Haltenbanken Area, in: Foster, N.H., Beaumont, E.A. (Eds.), Structural Traps VI, pp. 37-54.

Gradstein, F.M., Ogg, J.G., Schmitz, M., Ogg, G., 2012. The Geologic Time Scale 2012. Elsevier.

Greb, S.F., DiMichele, W.A., Gastaldo, R.A., 2006. Evolution and importance of wetlands in earth history, in: Greb, S.F., DiMichele, W.A. (Eds.), Wetlands through Time, Geol. Soc. Am. Spec. Pap., 399, pp. 1-40.

Gugliotta, M., Flint, S.S., Hodgson, D.M., Veiga, G.D., 2015. Stratigraphic Record of River-Dominated Crevasse Subdeltas With Tidal Influence (Lajas Formation, Argentina). J. Sed. Res. 85, 265-284.

Gugliotta, M., Kurcinka, C.E., Dalrymple, R.W., Flint, S.S., Hodgson, D.M., 2016. Decoupling seasonal fluctuations in fluvial discharge from the tidal signature in ancient deltaic deposits: an example from the Neuquén Basin, Argentina. J. Geol. Soc. 173, 94-107.

Hamm, L., Madsen, P.A., Peregrine, D.H., 1993. Special Issue Coastal Morphodynamics: Processes and Modelling Wave transformation in the nearshore zone: A review. Coast. Eng. 21, 5-39.

Hampson, G.J., 1997. A sequence stratigraphic model for deposition of the Lower Kinderscout Delta, an Upper Carboniferous turbidite-fronted delta. P. Yorks. Geol. Soc. 51, 273-296.

Hampson, G.J., Duller, R.A., Petter, A.L., Robinson, R.A.J., Allen, P.A., 2014. Mass-Balance Constraints On Stratigraphic Interpretation of Linked Alluvial–Coastal–Shelfal Deposits From Source To Sink: Example From Cretaceous Western Interior Basin, Utah and Colorado, U.S.A. J. Sed. Res. 84, 935-960.

Hampson, G.J., Gani, M.R., Sharman, K.E., Irfan, N., Bracken, B., 2011. Along-Strike and Down-Dip Variations in Shallow-Marine Sequence Stratigraphic Architecture: Upper Cretaceous Star Point Sandstone, Wasatch Plateau, Central Utah, U.S.A. J. Sed. Res. 81, 159-184.

Harris, N.B., 1989. Reservoir Geology of Fangst Group (Middle Jurassic), Heidrun Field, Offshore Mid-Norway. AAPG Bull. 73, 1415-1435.

Hartley, A.J., Owen, A., Swan, A., Weissmann, G.S., Holzweber, B.I., Howell, J., Nichols, G., Scuderi, L., 2016. Recognition and importance of amalgamated sandy meander belts in the continental rock record. Geology 44.

Helland-Hansen, W., Hampson, G.J., 2009. Trajectory analysis: concepts and applications. Basin Res. 21, 454-483.

Hinds, D.J., Aliyeva, E., Allen, M.B., Davies, C.E., Kroonenberg, S.B., Simmons, M.D., Vincent, S.J., 2004. Sedimentation in a discharge dominated fluvial-lacustrine system: the Neogene Productive Series of the South Caspian Basin, Azerbaijan. Mar. Pet. Geol. 21, 613-638.

Hine, A.C., Boothroyd, J.C., 1978. Morphology, processes, and recent sedimentary history of a glacial-outwash plain shoreline, southern Iceland. J. Sed. Res. 48, 901-920.

Ichaso, A.A., Dalrymple, R.W., 2014. Eustatic, tectonic and climatic controls on an early syn-rift mixed-energy delta, Tilje Formation (Early Jurassic, Smørbukk field, offshore mid-Norway), in: Martinius, A.W., Ravnås, R., Howell, J.A., Steel, R.J., Wonham, J.P. (Eds.), From Depositional Systems to Sedimentary Successions on the Norwegian Continental Margin, IAS Spec. Publ. 46, pp. 339-388.

Ichaso, A.A., Dalrymple, R.W., 2009. Tide- and wave-generated fluid mud deposits in the Tilje Formation (Jurassic), offshore Norway. Geology 37, 539-542.

Ichaso, A.A., Dalrymple, R.W., Martinius, A.W., 2016. Basin analysis and sequence stratigraphy of the synrift Tilje Formation (Lower Jurassic), Halten terrace giant oil and gas fields, offshore mid-Norway. AAPG Bull. 100, 1329-1375.

Jablonski, B.V.J., Dalrymple, R.W., 2016. Recognition of strong seasonality and climatic cyclicity in an ancient, fluvially dominated, tidally influenced point bar: Middle McMurray Formation, Lower Steepbank River, north-eastern Alberta, Canada. Sedimentology 63, 552-585.

Jacobsen, V.W., Van Veen, P., 1984. The Triassic offshore Norway north of 62°N, in: Spencer, A.M. (Ed.), Petroleum Geology of the North European Margin, Trondheim, pp. 317-327.

Johnson, H.D., 1975. Tide- and wave-dominated inshore and shoreline sequences from the late Precambrian, Finnmark, North Norway. Sedimentology 22, 45-74.

Keen, T.R., Slingerland, R.L., Bentley, S.J., Furukawa, Y., Teague, W.J., Dykes, J.D., 2012. Sediment Transport on Continental Shelves: Storm Bed Formation and Preservation in Heterogeneous Sediments, in: Li, M.Z., Sherwood, C.R., Hill, P.R. (Eds.), Sediments, Morphology and Sedimentary Processes on Continental Shelves: Advances in Technologies, Research, and Applications, IAS Spec. Publ. 44, pp. 295-310.

Korus, J.T., Fielding, C.R., 2015. Enhanced bioturbation on the down-drift flank of a Turonian asymmetrical delta: Implications for seaway circulation, river nutrients and facies models. Sedimentology 62, 1899-1922.

Kostaschuk, R.A., 1985. River mouth processes in a fjord-delta, British Columbia, Canada. Mar. Geol. 69, 1-23.

Kostaschuk, R.A., McCann, S.B., 1983. Observations on delta-forming processes in a fjord-head delta, British Columbia, Canada. Sediment. Geol. 36, 269-288.

Kroonenberg, S.B., Alekseevski, N.I., Aliyeva, E., Allen, M.B., Aybulatov, D.N., Baba-Zadeh, A., Badyukova, E.N., Davies, C.E., Hinds, D.J., Hoogendoorn, M.B., Huseynov, D., Ibrahimov, B., Mamedov, P., Overeem, I., Rusakov, G.V., Suleymanova, S., Svitoch, A.A., Vincent, S.J., 2005. Two deltas, two basins, one river, one sea: The modern Volga delta as an analogue of the Neogene Productive Series, South Caspian Basin, in: Giosan, L., Bhattacharya, J.P. (Eds.), River Deltas-Concepts, Models, and Examples, pp. 231-256.

Kroonenberg, S.B., Rusakov, G.V., Svitoch, A.A., 1997. The wandering of the Volga delta: a response to rapid Caspian sea-level change. Sediment. Geol. 107, 189-209.

Leeder, M.R., Gawthorpe, R.L., 1987. Sedimentary models for extensional tilt-block/half-graben basins, in: Coward, M.P., Dewey, J.F., Hancock, P.L. (Eds.), Continental Extensional Tectonics, Geol. Soc. Spec. Publ. 28, pp. 139-152.

Leeder, M., 1973. Sedimentology and palaeogeography of the Upper Old Red Sandstone in the Scottish Border Basin. Scot. J. Geol. 9, 117-144.

Legler, B., Hampson, G.J., Jackson, C.A.L., Johnson, H.D., Massart, B.Y.G., Sarginson, M., Ravnås, R., 2014. Facies Relationships and Stratigraphic Architecture of Distal, Mixed Tide- and Wave-Influenced Deltaic Deposits: Lower Sego Sandstone, Western Colorado, U.S.A. J. Sed. Res. 84, 605-625.

Li, W., Bhattacharya, J.P., Zhu, Y., Garza, D., Blankenship, E., 2011. Evaluating delta asymmetry using three-dimensional facies architecture and ichnological analysis, Ferron 'Notom Delta', Capital Reef, Utah, USA. Sedimentology 58, 478-507.

Li, Z., Bhattacharya, J., Schieber, J., 2015. Evaluating along-strike variation using thin-bedded facies analysis, Upper Cretaceous Ferron Notom Delta, Utah. Sedimentology 62, 2060-2089.

MacEachern, J.A., Raychaudhuri, I., Pemberton, S.G., 1992. Stratigraphic applications of the *Glossifungitis* ichnofacies: delineating discountinuities in the rock record, in: Pemberton, S.G. (Ed.), Applications of Ichnology to Petroleum Exploration, Core Workshop 17, pp. 169-198.

MacEachern, J.A., Bann, K.L., 2008. The Role of Ichnology in Refining Shallow Marine Facies Models, in: Hampson, G.J., Steel, R.J., Burgess, P.M., Dalrymple, R.W. (Eds.), Recent Advances in Models of Siliciclastic Shallow-Marine Stratigraphy, SEPM Spec. Publ. 90, pp. 73-116.

Marsh, N., Imber, J., Holdsworth, R.E., Brockbank, P., Ringrose, P., 2010. The structural evolution of the Halten Terrace, offshore Mid-Norway: extensional fault growth and strain localisation in a multi-layer brittle-ductile system. Basin Res. 22, 195-214.

Martinius, A.W., Ringrose, P.S., Brostrøm, C., Elfenbein, C., Næss, A., Ringås, J.E., 2005. Reservoir challenges of heterolithic tidal sandstone reservoirs in the Halten Terrace, mid-Norway. Petrol. Geosci. 11, 3-16.

Martinius, A.W., Kaas, I., Næss, A., Helgesen, G., Kjærefjord, J.M., Leith, D.A., 2001. Sedimentology of the heterolithic and tide-dominated Tilje Formation (Early Jurassic, Halten Terrace, Offshore Mid-Norway), in: Martinsen, O.J., Dreyer, T. (Eds.), Sedimentary Environments Offshore Norway: Palaeozoic to Recent, Norwegian Petroleum Society Spec. Publ. 10, pp. 103-144.

Martinsen, O.J., Lien, T., Jackson, C., 2005. Cretaceous and Palaeogene turbidite systems in the North Sea and Norwegian Sea Basins: source, staging area and basin physiography controls on reservoir development, in: Doré, A.G., Vining, B.A. (Eds.), Petroleum Geology: North-West Europe and Global Perspective, pp. 1147-1164.

McIlroy, D., 2004. Ichnofabrics and sedimentary facies of a tide-dominated delta: Jurassic Ile Formation of the Kristin Field, Haltenbanken, Offshore Mid-Norway, in: McIlroy, D. (Ed.), The Application of Ichnology to Palaeoenvironmental and Stratigraphic Analysis, pp. 237-272.

McIlroy, D., Flint, S., Howell, J.A., Timms, N., 2005. Sedimentology of the tide-dominated Jurassic Lajas Formation, Neuquén Basin, Argentina, in: Veiga, G.D., Spalletti, L.A., Howell, J.A., Schwarz, E. (Eds.), The Neuquen Basin, Argentina: A Case Study in Sequence Stratigraphy and Basin Dynamics, Geol. Soc. London Spec. Publ. 252, pp. 83-107.

McPherson, J.G., Shanmugam, G., Moiola, R.J., 1987. Fan-deltas and braid deltas: Varieties of coarse-grained deltas. Geol. Soc. Am. Bull. 99, 331-340.

Meor, H.A.H., Johnson, H.D., Allison, P.A., Abdullah, W.H., 2013. Sedimentology and stratigraphic development of the upper Nyalau Formation (Early Miocene), Sarawak, Malaysia: A mixed wave- and tide-influenced coastal system. J. Asian Earth Sci. 76, 301-311.

Messina, C., Nemec, W., Martinius, A.W., Elfenbein, C., 2014. The Garn Formation (Bajocian-Bathonian) in the Kristin Field, Halten Terrace, in: Martinius, A.W., Ravnås, R., Howell, J.A., Steel, R.J., Wonham, J.P. (Eds.), From Depositional Systems to Sedimentary Successions on the Norwegian Continental Margin, IAS Spec. Publ. 46, pp. 513-550.

Miall, A.D., 1996. The Geology of Fluvial Deposits: Sedimentary Facies, Basin Analysis, and Petroleum Geology. Springer, Berlin Heidelberg.

Miall, A.D., 1991. Stratigraphic sequences and their chronostratigraphic correlation. J. Sed. Res. 61, 497-505.

Michael, N.A., Whittaker, A.C., Allen, P.A., 2013. The Functioning of Sediment Routing Systems Using a Mass Balance Approach: Example from the Eocene of the Southern Pyrenees. J. Geol. 121, 581-606.

Morton, A., Hallsworth, C., Strogen, D., Whitham, A., Fanning, M., 2009. Evolution of provenance in the NE Atlantic rift: The Early–Middle Jurassic succession in the Heidrun Field, Halten Terrace, offshore Mid-Norway. Mar. Pet. Geol. 26, 1100-1117.

Muto, T., 2001. Shoreline Autoretreat Substantiated in Flume Experiments. J. Sed. Res. 71, 246-254.

Muto, T., Steel, R.J., 2001. Autostepping during the transgressive growth of deltas: Results from flume experiments. Geology 29, 771-774.

Muto, T., Steel, R.J., 1997. Principles of regression and transgression; the nature of the interplay between accommodation and sediment supply. J. Sed. Res. 67, 994-1000.

Muto, T., Steel, R.J., 1992. Retreat of the front in a prograding delta. Geology 20, 967-970.

Muto, T., Steel, R.J., Swenson, J.B., 2007. Autostratigraphy: A Framework Norm for Genetic Stratigraphy. J. Sed. Res. 77, 2-12.

Nageswara Rao, K., Sadakata, N., Hema Malini, N., Takayasu, K., 2005. Sedimentation processes and asymmetric development of the Godavari delta, India, in: Giosan, L., Bhattacharya, J.P. (Eds.), River Deltas-Concepts, Models, and Examples, SEPM Spec. Publ. 83, pp. 435-451.

Nageswara Rao, K., Saito, Y., Nagakumar, K.C.V., Demudu, G., Rajawat, A.S., Kubo, S., Li, Z., 2015. Palaeogeography and evolution of the Godavari delta, east coast of India during the Holocene: An example of wave-dominated and fan-delta settings. Palaeogeogr. , Palaeoclimatol. , Palaeoecol. 440, 213-233.

Nemec, W., Postma, G., 1993. Quaternary alluvial fans in southwestern Crete: sedimentation processes and geomorphic evolution, in: Marzo, M., Puigdefábregas, C. (Eds.), Alluvial Sedimentation, IAS Spec. Publ. 17, pp. 235-276.

Norwegian Petroleum Directorate (NPD), 2016. FactMaps. www.npd.no.

Nøttvedt, A., Johannessen, E.P., Surlyk, F., 2008. The Mesozoic of Western Scandinavia and East Greenland. Episodes 31, 59-65.

Olariu, C., 2014. Autogenic process change in modern deltas: lessons for the ancient, in: Martinius, A.W., Ravnås, R., Howell, J.A., Steel, R.J., Wonham, J.P. (Eds.), From Depositional Systems to Sedimentary Successions on the Norwegian Continental Margin, IAS Spec. Publ. 47, pp. 149-166.

Orton, G.J., Reading, H.G., 1993. Variability of deltaic processes in terms of sediment supply, with particular emphasis on grain size. Sedimentology 40, 475-512.

Overeem, I., Kroonenberg, S.B., Veldkamp, A., Groenesteijn, K., Rusakov, G.V., Svitoch, A.A., 2003. Small-scale stratigraphy in a large ramp delta: recent and Holocene sedimentation in the Volga delta, Caspian Sea. Sediment. Geol. 159, 133-157.

Pemberton, S.G., Gingras, M.K., Dashgard, S.E., Bann, K.L., MacEachern, J., 2009. The *Teichichnus* Ichnofacies: a Temporally and Spatially Recurring Ethological Grouping Characteristic of Brackish-Water Conditions. AAPG Annual Convention and Exhibition, Denver, Colorado .

Penland, S., Boyd, R., Suter, J.R., 1988. Transgressive depositional systems of the Mississippi Delta plain; a model for barrier shoreline and shelf sand development. J. Sed. Res. 58, 932-949.

Posamentier, H.W., Morris, W.R., 2000. Aspects of the stratal architecture of forced regressive deposits, in: Hunt, D., Gawthorpe, R.L. (Eds.), Sedimentary Responses to Forced Regressions, Geol. Soc. London Spec. Publ. 172, pp. 19-46.

Prince, G.D., Burgess, P.M., 2013. Numerical Modeling of Falling-Stage Topset Aggradation: Implications for Distinguishing Between Forced and Unforced Regressions In the Geological Record. J. Sed. Res. 83, 767-781.

Provan, D.M.J., 1992. Draugen Oil Field, Haltenbanken Province, Offshore Norway, in: Halbouty, M.T. (Ed.), Giant Oil and Gas Fields of the Decade 1978-1988, pp. 371-382.

Ravnås, R., Nøttvedt, A., Steel, R.J., Windelstad, J., 2000. Syn-rift sedimentary architectures in the Northern North Sea, in: Nøttvedt, A. (Ed.), Dynamics of the Norwegian Margin, Geol. Soc. Spec. Publ. 167, pp. 133-177.

Ravnås, R., Berge, K., Campbell, H., Harvey, C., Norton, M.J., 2014. Halten Terrace Lower and Middle Jurassic inter-rift megasequence analysis: megasequence structure, sedimentary architecture and controlling parameters, in: Martinius, A.W., Ravnås, R., Howell, J.A., Steel, R.J., Wonham, J.P. (Eds.), From Depositional Systems to Sedimentary Successions on the Norwegian Continental Margin, IAS Spec. Publ. 46, pp. 215-252.

Ravnås, R., Steel, R.J., 1998. Architecture of marine rift-basin successions. AAPG Bull. 82, 110-146.

Reineck, H.E., 1958. Longitudinale Schrägschicht im Watt. Geol. Rundsch. 47, 73-82.

Reineck, H.E., Wunderlich, F., 1968. Classification and origin of flaser and lenticular bedding. Sedimentology 11, 99-104.

Richardson, N.J., Underhill, J.R., Lewis, G., 2005. The role of evaporite mobility in modifying subsidence patterns during normal fault growth and linkage, Halten Terrace, Mid-Norway. Basin Res. 17, 203-223.

Robinson, R.A.J., Slingerland, R.L., 1998. Grain-size trends, basin subsidence and sediment supply in the Campanian Castlegate Sandstone and equivalent conglomerates of central Utah. Basin Res. 10, 109-127.

Rohais, S., Eschard, R., Guillocheau, F., 2008. Depositional model and stratigraphic architecture of rift climax Gilbert-type fan deltas (Gulf of Corinth, Greece). Sediment. Geol. 210, 132-145.

Rossi, V.M., Steel, R.J., 2016. The role of tidal, wave and river currents in the evolution of mixed-energy deltas: Example from the Lajas Formation (Argentina). Sedimentology 63, 824-864.

Salahuddin, Lambiase, J.J., 2013. Sediment Dynamics and Depositional Systems of the Mahakam Delta, Indonesia: Ongoing Delta Abandonment On A Tide-Dominated Coast. J. Sed. Res. 83, 503-521.

Scott, E.S., 1992. The palaeoenvironments and dynamics of the Rannoch—Etive nearshore and coastal succession, Brent Group, northern North Sea, in: Morton, A.C., Haszeldine, R.S., Giles, R.S., Browns, S. (Eds.), Geology of the Brent Group, Geol. Soc. Spec. Publ. 61, pp. 129-147.

Soil Survey Staff, 1999. Soil Taxonomy A Basic System of Soil Classification for Making and Interpreting Soil Surveys. United States Department of Agriculture, Washington, DC.

Sømme, T.O., Jackson, C.A.L., 2013. Source-to-sink analysis of ancient sedimentary systems using a subsurface case study from the Møre-Trøndelag area of southern Norway: Part 2 – sediment dispersal and forcing mechanisms. Basin Res. 25, 512-531.

Sømme, T.O., Martinsen, O.J., Lunt, I., 2013. Linking offshore stratigraphy to onshore paleotopography: The Late Jurassic–Paleocene evolution of the south Norwegian margin. Geol. Soc. Am. Bull. 125, 1164-1186.

Strong, N., Sheets, B., Hickson, T., Paola, C., 2005. A mass-balance framework for quantifying downstream changes in fluvial architecture, in: Blum, M., Marriott, S., Leclair, S. (Eds.), Fluvial Sedimentology VII, IAS Spec. Publ. 35, pp. 243-253.

Surlyk, F., 1990. Timing, style and sedimentary evolution of Late Palaeozoic-Mesozoic extensional basins of East Greenland, in: Hard, R.F.P., Brooks, J. (Eds.), Tectonic Events Responsible for Britain's Oil and Gas Reserves, Geol. Soc. Spec. Publ. 55, pp. 107-125.

Syvitski, J.P.M., Farrow, G.E., 1983. Structures and processes in bayhead deltas: Knight and bute inlet, British Columbia. Sediment. Geol. 36, 217-244.

Taylor, A.M., Goldring, R., 1993. Description and analysis of bioturbation and ichnofabric. J. Geol. Soc. 150, 141-148.

Terwindt, J.H.J., 1971. Litho-facies of inshore estuarine and tidal-inlet deposits. Geol. Mijnbouw 50, 515-526.

Thomas, R.G., Smith, D.G., Wood, J.M., Visser, J., Calverley-Range, E.A., Koster, E.H., 1987. Inclined heterolithic stratification—Terminology, description, interpretation and significance. Sed. Geol. 53, 123-179.

Thrana, C., Næss, A., Leary, S., Gowland, S., Brekken, M., Taylor, A., 2014. Updated depositional and stratigraphic model of the Lower Jurassic Åre Formation, Heidrun Field, Norway, in: Martinius, A.W., Ravnås, R., Howell, J.A., Steel, R.J., Wonham, J.P. (Eds.), From Depositional Systems to Sedimentary Successions on the Norwegian Continental Margin, IAS Spec. Publ. 46, pp. 253-289.

Vakarelov, B.K., Ainsworth, R.B., 2013. A hierarchical approach to architectural classification in marginal-marine systems: Bridging the gap between sedimentology and sequence stratigraphy. AAPG Bull. 97, 1121-1161.

Vakarelov, B.K., Ainsworth, R.B., MacEachern, J.A., 2012. Recognition of wave-dominated, tide-influenced shoreline systems in the rock record: Variations from a microtidal shoreline model. Sed. Geol. 279, 23-41.

Van Cappelle, M., Stukins, S., Hampson, G.J., Johnson, H.D., 2016. Fluvial to tidal transition in proximal, mixed tide-influenced and wave-influenced deltaic deposits: Cretaceous lower Sego Sandstone, Utah, USA. Sedimentology 63, 1333-1361.

Van den Berg, J.H., Boersma, J.R., Van Gelder, A., 2007. Diagnostic sedimentary structures of the fluvial-tidal transition zone - Evidence from deposits of the Rhine and Meuse. Neth. J. Geosci. 86, 387-306.

Van Straaten, L.M.J.U., Kuenen, P.H., 1957. Accumulation of fine grained sediments in the Dutch Wadden Sea. Geol. Mijnbouw 19, 329-354.

Vosgerau, H., Alsen, P., Carr, I.D., Therkelsen, J., Stemmerik, L., Surlyk, F., 2004. Jurassic syn-rift sedimentation on a seawards-tilted fault block, Traill Ø, North-East Greenland. Geol. Surv. Den. Greenl. 5, 9-18.

Walker, R.G., 1966. Shale Grit and Grindslow shales; transition from turbidite to shallow water sediments in the upper Carboniferous of northern England. J. Sed. Res. 36, 90-114.

Wei, X., Steel, R.J., Ravnås, R., Jiang, Z., Olariu, C., Li, Z., 2016. Variability of tidal signals in the Brent Delta Front: New observations on the Rannoch Formation, northern North Sea. Sediment. Geol. 335, 166-179.

Willis, B.J., Gabel, S.L., 2003. Formation of Deep Incisions into Tide-Dominated River Deltas: Implications for the Stratigraphy of the Sego Sandstone, Book Cliffs, Utah, U.S.A. J. Sed. Res. 73, 246-263.

Willis, B.J., Gabel, S.L., 2001. Sharp-based, tide-dominated deltas of the Sego Sandstone, Book Cliffs, Utah, USA. Sedimentology 48, 479-506.

Wilson, P., Elliott, G.M., Gawthorpe, R.L., Jackson, C.A.-., Michelsen, L., Sharp, I.R., 2013. Geometry and segmentation of an evaporite-detached normal fault array: 3D seismic analysis of the southern Bremstein Fault Complex, offshore mid-Norway. J. Struct. Geol. 51, 74-91.

Wright, L.D., 1977. Sediment transport and deposition at river mouths: A synthesis. Geol. Soc. Am. Bull. 88, 857-868.

Yang, B.C., Dalrymple, R.W., Chun, S.S., 2005. Sedimentation on a wave-dominated, open-coast tidal flat, south-western Korea: summer tidal flat - winter shoreface. Sedimentology 52, 235-252.

Yoshida, S., Steel, R.J., Dalrymple, R.W., 2007. Changes in Depositional Processes—An Ingredient in a New Generation of Sequence-Stratigraphic Models. J. Sed. Res. 77, 447-460.

Ziegler, P.A., 1988. Evolution of the Arctic - North Atlantic and the Western Tethys. AAPG Memoir 43.

**Figure 1. (A) Palaeogeographic map of northern Europe and surrounding areas during the Middle Jurassic (~170 Ma) showing the context of the Halten Terrace (modified after Ziegler, 1988; Doré, 1992; Engkilde and Surlyk, 2003; Ravnås et al., 2014; Eide et al., 2016). (B) Map showing the main structural elements of the Halten Terrace (modified after Blystad et al., 1995). (C) Map of the study area showing the locations of the wells and well correlations panels used in this study (Norwegian Petroleum Directorate (NPD), 2016).**

**Figure 2. Lithostratigraphy of the Late Triassic to Early Cretaceous of the Halten Terrace (modified after Dalland et al., 1988; Gradstein et al., 2012; Ravnås et al., 2014).**

**Figure 3. Summary graphical table of facies and facies associations. Lithology abbreviations: vf.=very fine; f.=fine; m.=medium; c.=coarse; vc.=very coarse; m.=muddy; mst.=mudstone; hl.=heterolithic; s.=sandy; sst.=sandstone; p.=pebbly; cgl.=conglomerate. Trace fossil abbreviations: as.=*Asterosoma*; Carb. Debris=carbonaceous debris, co.=*Cosmorhaphe*; cr.=*Cruziana*; cy.=*Cylindrichnus*; e.t.=escape trace, gy.=*Gyrochorte*; he.=*Helminthopsis*; lo.=*Lockeia*; op.=*Ophiomorpha*; pa.=*Palaeophycus*; pl.=*Planolites*; ro.=*Rosellia*; sc.=*Schaubcylindrichnus*; sk.=*Skolithos*; sl.=*Scolicia*; te.=*Teichichnus*; th.=*Thalassinoides*; zo.=*Zoophycos*; WF.= wireline log facies.**

**Figure 4. Panel showing photographs of facies associations FA1-FA4, which typically occur together in upward-coarsening facies successions, colour coded by facies association (Figure 3). For abbreviations see Figure 3. (A) Poorly sorted cross-bedded fluvial sandstone (facies F3b; well 6406/9-3 4730 m). (B) Very poorly sorted cross-bedded pebbly fluvial sandstone (facies F3a; well 6406/9-3 4727 m). (C) Very poorly sorted cross-bedded pebbly sandstone with *Skolithos* (faciesF4a; well 6406/9-1 4617 m). (D) Two cross-bedded coarse-grained sandstones beds (indicating high fluvial discharge, facies F4b) separated by a heterolithic fine-grained sandstone bed with bioturbation (indicating tidal and marine reworking, facies F4c; well 6406/9-1 4608 m). (E) Hummocky cross-stratified very fine-grained sandstone with interbedded siltstone and sandstone lenses (facies F2a; well 6406/9-1 4784 m). (F) Current ripple cross-laminated sandstone (facies F2b; well 6406/5-1 4506 m). (G) Current ripple cross-laminated (facies F2b) and cross-bedded sandstone (facies F2d; well 6406/5-1 4507 m). (H-J) Heterolithic bioturbated offshore mudstones (facies F1d; H, well 6406/5-1 4522 m; I, well 6406/9-1 4855 m; J, well 6406/9-1 4856 m). (K) Laminations, combined flow ripples and current ripples (facies F1b; well 6406/9-1 4798m). (L) Combined flow ripples forming very fine-grained sandstones lenses in prodelta mudstone (facies F1b; well 6406/9-1 4803 m).**

**Figure 5. Panel showing photographs of facies associations FA5 and FA7, and related erosional surfaces, colour coded by facies association (Figure 3). For abbreviations see Figure 3. (A) Erosional surface overlain by a lag of quartz pebbles and 1-10 cm wide mud chips (facies F4a; well 6406/8-1 4464 m). (B) Sharp based sandstones with mud draped cross-bedding (facies F5c) and mud-draped cross-lamination (facies F5b) and homogenous mudstones (facies F5a; well 6407/6-5 2512**

**m). Mud drapes are indicated with black arrows, homogenous mudstones interpreted as fluid muds are indicated with white arrows labelled 'fm'. (C) Apparent bidirectional, mud-draped, cross-laminated, heterolithic sandstones with bioturbation (facies F5b; well 6407/6-5 2510 m). (D) Muddy sandstone with rootlets (facies F7b) overlain by a coal bed (F7c; 6407/10-2 3447 m). (E) *Thalassinoides* burrows constituting a *Glossifungitis* ichnofacies, that marks a firmground surface (facies F6d; well 6407/6-3 2589 m). (F) Homogenous mudstone with synaeresis cracks sharply overlain by cross-laminated sandstone (facies F5a; well 6407/6-5 2553 m). (G) Thin coal horizon with rootlets penetrating the underlying sandstone (facies F7c; 6407/10-2 3454 m).**

**Figure 6. Core photographs of facies association FA6 (tidal coastline). (A) Overview 3 m interval containing alternations of facies F6a (dark blue) and F6b (light blue; well 6406/5-1). (B) Undulatory and planar laminated sandstones of (facies F6a, well 6406/8-1 4409 m). (C) Apparent bidirectional cross-lamination with mud drapes (facies F6b; well 6406/5-1 4357 m).**

**Figure 7. (A,C) Example core logs through upward-shallowing, progradational successions of facies associations FA1, FA2, FA3 and FA4 in wells 6407/6-3 and 6406/9-2. (B,D) Example core logs through aggradational successions of facies associations FA5, FA6 and FA7 in wells 6407/10-2 and 6407/6-5.**

**Figure 8. Example well (6407/6-5) showing the three vertical facies succession that are used to subdivide the studied strata into stratigraphic intervals.**

**Figure 9. Correlation panel with north-south (A-C) and west-east (D-F) orientations. For location see Figure 1C.**

**Figure 10. Maps for stratigraphic intervals progradational phase I, progradational phase II and aggradational phase III (Fig. 8): (A) isopach of total thickness for progradational phase I; (B) extent of condensed section marked by high GR values in basal part of progradational phase I; (C) sandstone thickness (FA2, FA3, FA4) for progradational phase I, with inferred sediment supply routes (black arrows); (D) channel-fill deposit (FA3, FA4) thickness for progradational phase I, with inferred sediment supply routes (black arrows); (E) isopach of total thickness for progradational phase II; (F) proportions of wireline log facies in each well (pie charts) for progradational phase II, and highlighting areas of gradational and "sharp-based" delta-front successions; (G) isopach map of aggradational phase III; (H) proportions of wireline log facies in each well (pie charts) for aggradational phase III.**

**Figure 11. Depositional models (A,C) and interpreted process regime (B,D, modified after Ainsworth et al., 2011) for progradational phases I and II (A,B) and aggradational phase III (C,D). The placement of the facies associations in the terniary diagram represents the interpreted mix of depositional processes of the facies association. The black circles indicate the overall process regimes of the depositional environments in which the facies associations have been**

**interpreted to be deposited (mixed wave- and/or fluvial-dominated, tide-influenced delta; tide-dominated, fluvial influenced delta; and tide-dominated coastline).**

**Figure 12. A) Map synthesising the interpreted location and size of the "Tofte and Ile sediment routing systems", from their erosional source areas to their depositional sinks (Gjelberg et al., 1987; Ziegler, 1988; Surlyk, 1990; Doré, 1992; Alsgaard et al., 2003; Vosgerau et al., 2004; Nøttvedt et al., 2008; Elliott et al., 2012; Sømme et al., 2013; Sømme and Jackson, 2013; Ravnås et al., 2014; Elliott et al., 2015; Eide et al., 2016). (B) Sketch cross-section illustrating the potential thickness of the principal "Tofte and Ile sediment routing system" along the major axial depositional system, as required to explain the overall progradational-aggradational-retrogradational architecture of the associated strata via autoretreat. Grain size distributions expected from mass-balance consideration of this cross-section are also shown. (C, D) Expanded view of the distal part of Figure 12B showing grain size distributions (C) and stratal architecture and facies-association distributions (D) in the study area and adjacent areas.**

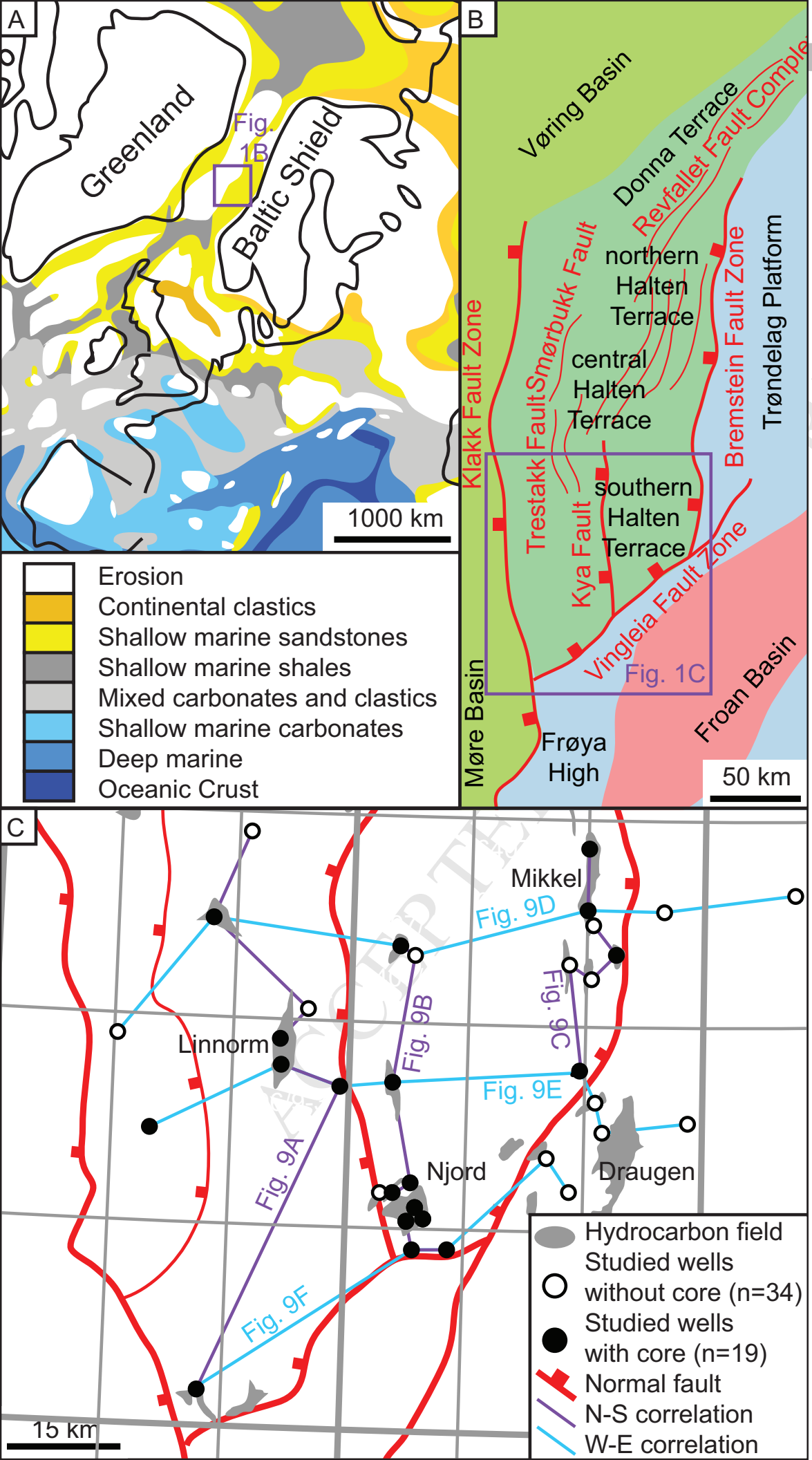
A
Greenland
Fig. 1B
Baltic Shield
1000 km
Erosion
Continental clastics
Shallow marine sandstones
Shallow marine shales
Mixed carbonates and clastics
Shallow marine carbonates
Deep marine
Oceanic Crust
B
Vøring Basin
Donna Terrace
Revfallet Fault Complex
Klakk Fault Zone
Smørbukk Fault
northern Halten Terrace
central Halten Terrace
Trestakk Fault
Kya Fault
southern Halten Terrace
Bremstein Fault Zone
Trøndelag Platform
Vingleia Fault Zone
Fig. 1C
Møre Basin
Frøya High
Froan Basin
50 km
C
Mikkel
Fig. 9D
Fig. 9C
Fig. 9B
Linnorm
Fig. 9E
Fig. 9A
Njord
Draugen
Fig. 9F
15 km
Hydrocarbon field
Studied wells without core (n=34)
Studied wells with core (n=19)
Normal fault
N-S correlation
W-E correlation

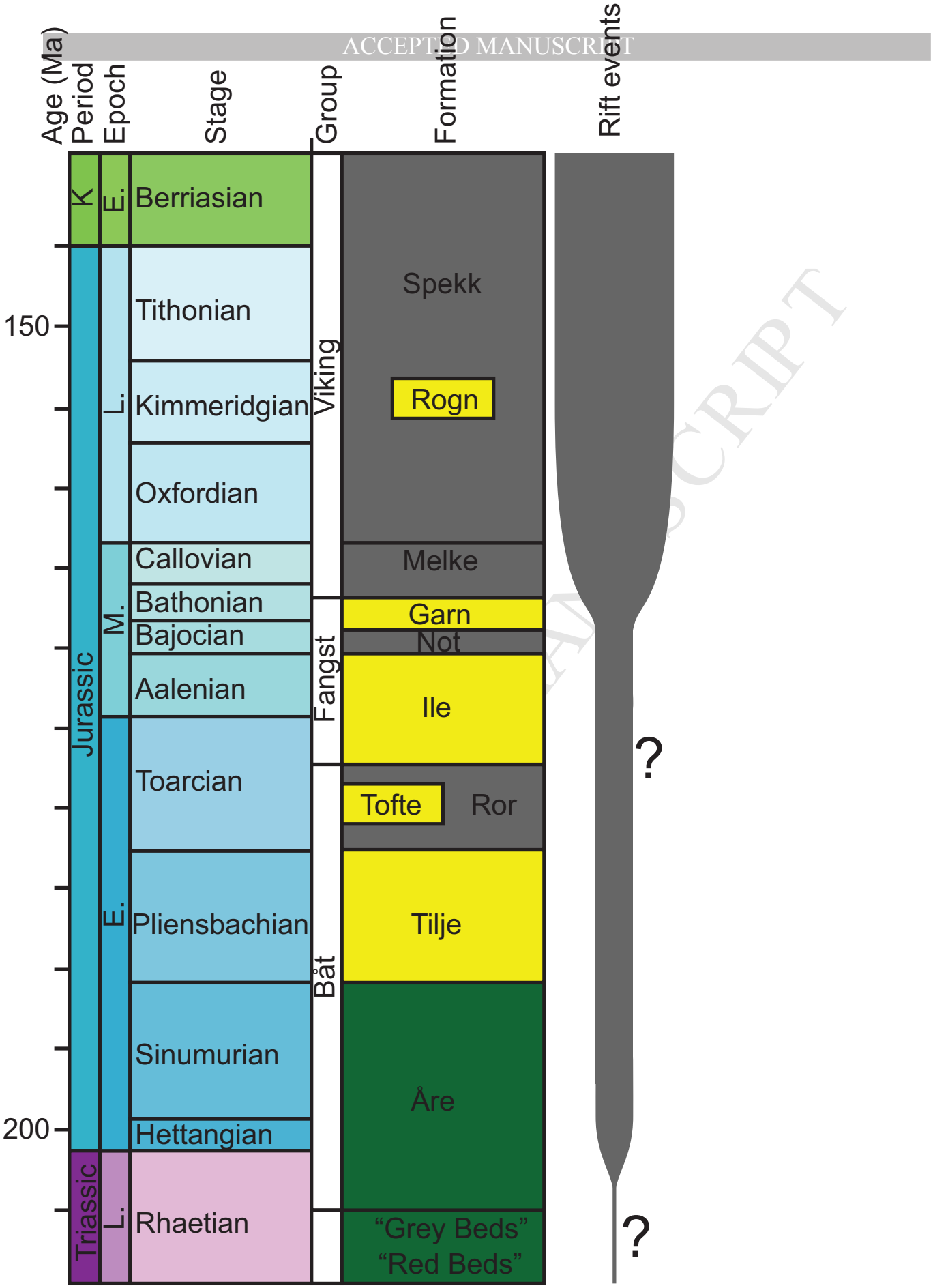

| Facies | FA. | Virtual log | Lithology | Physical structures | Trace and body fossils | Ichno-facies | BI | Interpretation | WF. |
|---|---|---|---|---|---|---|---|---|---|
| F8b | FA8 | 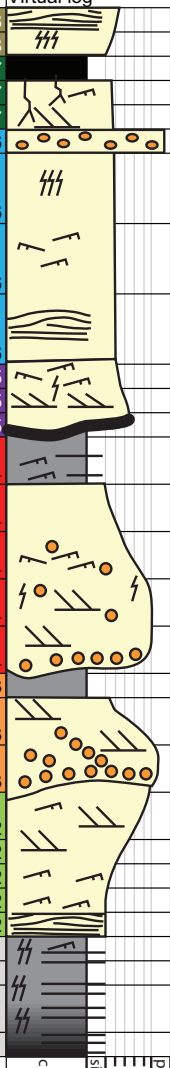 | vf. - f. sst. | Hummocky cross stratification | pl. pa. sc. th. te. sk. cy. lo. op. | Cr.-Sk. | 0-3 | Lower shoreface | LSF |
| F8a | FA8 | | vf. - f. sst. | | pl. pa. sc. th. te. sk. cy. lo. op. | Cr.-Sk. | 4-5 | Lower shoreface | |
| F7c | FA7 | | coal | | | | 0 | Coal mire | CM |
| F7b | FA7 | | vf. - f. hl. sst. | Cross lamination | rootlets, carb. debris, pl. cy. te. | Cr.-Sk. | 0-3 | Coal mire | |
| F7a | FA7 | | vf. - f. sst. | Cross bedding | rootlets, carb. debris, pl. cy. te. | Cr.-Sk. | 0-3 | Coal mire | |
| F6d | FA6 | | p. mst. - m. cgl | | th. | Gl. | 0 | Winnowed lag | HFSS |
| F6c | FA6 | | vf. - f. hl. sst. | | e.t. pa. pl. th. op. cy. te. sk. lo. sc. as. ro. | Cr.-Sk. | 4-5 | Tidal coastline | |
| F6b | FA6 | | vf. - f. hl. sst. | Bidirectional cross lamination and currents ripples, mud drapes | e.t. pa. pl. th. op. cy. te. sk. lo. sc. as. ro. | Cr.-Sk. | 0-3 | Tidal coastline | |
| F6a | FA6 | | vf. - f. hl. sst. | Micro-HCS (10 cm thick beds), and low angle cross lamination (10cm thick beds) | e.t. pa. pl. th. op. cy. te. sk. lo. sc. as. ro. | Cr.-Sk. | 0-3 | Tidal coastline | |
| F5c | FA5 | | f. sst. | Bidirectial current ripples, mud drapes, mud chips | e.t. lo. gy. op. pa. pl. cy. as. | Cr.-Sk. | 0-4 | Tidal channel | |
| F5b | FA5 | | f. - m. sst. | Cross bedded, draped foresets, mud chips | e.t. lo. gy. op. pa. pl. cy. as. | Cr.-Sk. | 0-4 | Tidal channel | |
| F5a | FA5 | | mst. | Homogenous, cm scale fluid mudstone | pa. pl. | Cr. | 0-1 | Tidal channel | |
| F4e | FA4 | | mst. | Current ripples, sand lenses | pa. pl. te. | Te. | 0-3 | Abandoned marine-influenced channel | CSS |
| F4d | FA4 | | m. - c. sst | Very well sorted, homogenous, cross bedding sometimes discernable, fluid mudstones | pa. pl | Cr. | 0-1 | Wave-influenced fluvial bar | |
| F4c | FA4 | | f. sst. | Irregular mud drapes, cross lamination | pa. cy. | Sk. | 2-3 | Marine-influenced channel | |
| F4b | FA4 | | f. - m. sst. | Cross bedding, cross lamination, fluid muds in toesets, mud chips lining foresets | pa. cy. | Sk. | 0-3 | Marine-influenced channel | |
| F4a | FA4 | | p. c. - vc. sst | Poorly sorted, cross bedded, mud clasts, granule and small pebble clasts | op. sk. cy. | Sk. | 1 | Marine-influenced channel | |
| F3c | FA3 | | Mst | Homogenous | | | 0 | Abandoned channel | |
| F3b | FA3 | | p. m. - vc. sst | Cross bedded, granule lags and granules lining foresets | | | 0 | Fluvial channel | |
| F3a | FA3 | | p. m. - vc. sst | Poorly sorted, floating granules and pebbles, and granule and pebble lags | | | 0 | Fluvial channel | |
| F2e | FA2 | | p. m. - vc. sst | Cross laminations, cross bedding, mud clasts, draped foresets | pa. pl. sk. | Cr.-Sk. | 0-1 | Mouth bar | DF |
| F2d | FA2 | | m. - c. sst. | Cross bedding | Carb. debris, pa. op. pl. ro. | Cr.-Sk. | 0-2 | Mouth bar | |
| F2c | FA2 | | vf. - f. sst. | Cross lamination and current ripples, fluid muds | pl. pa. op. ro. he. te. sc. th. | Cr.-Sk. | 2-5 | Delta front | |
| F2b | FA2 | | f. - m. sst. | Cross lamination and current ripples | Carb. debris | | 0 | Delta front | |
| F2a | FA2 | | vf. sst. | Hummocky cross stratification | e.t. pl. pa. | Cr.-Sk. | 0-1 | Delta front | |
| F1d | FA1 | | s. mst. | Rare current ripples | pl. pa. sc. he. op. th. te. sl. zo. | Cr. | 2-5 | Offshore | OS |
| F1c | FA1 | | s. mst. | | Carb. debris, sc. pa. co. | Cr. | 3-4 | Prodelta/Offshore | |
| F1b | FA1 | | mst. | Siltstone and very fine grained sandstones combined flow ripples | pl. sc. te. | Cr. | 1-3 | Prodelta | |
| F1a | | | mst. | | pl. sc. te. | | 0-1 | Prodelta | |
| | | clay silt sand pebble | | | | | | Condensed section on the shelf | CC |

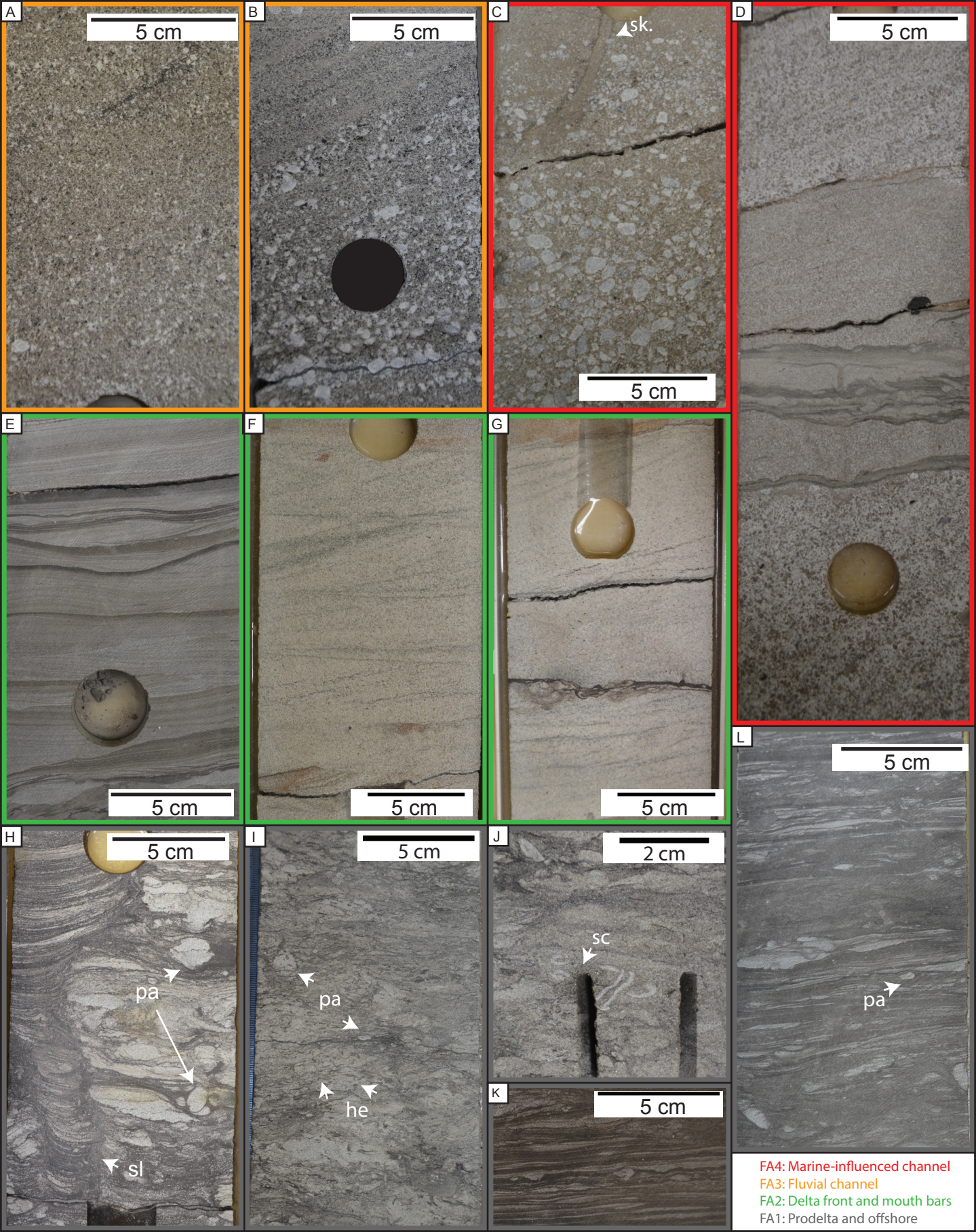
A
5 cm
B
5 cm
C
sk.
5 cm
D
5 cm
E
5 cm
F
5 cm
G
5 cm
L
5 cm
pa
H
5 cm
pa
sl
I
5 cm
pa
he
J
2 cm
sc
K
5 cm
FA4: Marine-influenced channel
FA3: Fluvial channel
FA2: Delta front and mouth bars
FA1: Prodelta and offshore


A
5 cm
B
5 cm
pa
fm
fm
fm
C
pa
as
5 cm
D
5 cm
E
5 cm
gl
F
5 cm
G
5 cm
FA7: Coal mire
FA5: Tidal channel

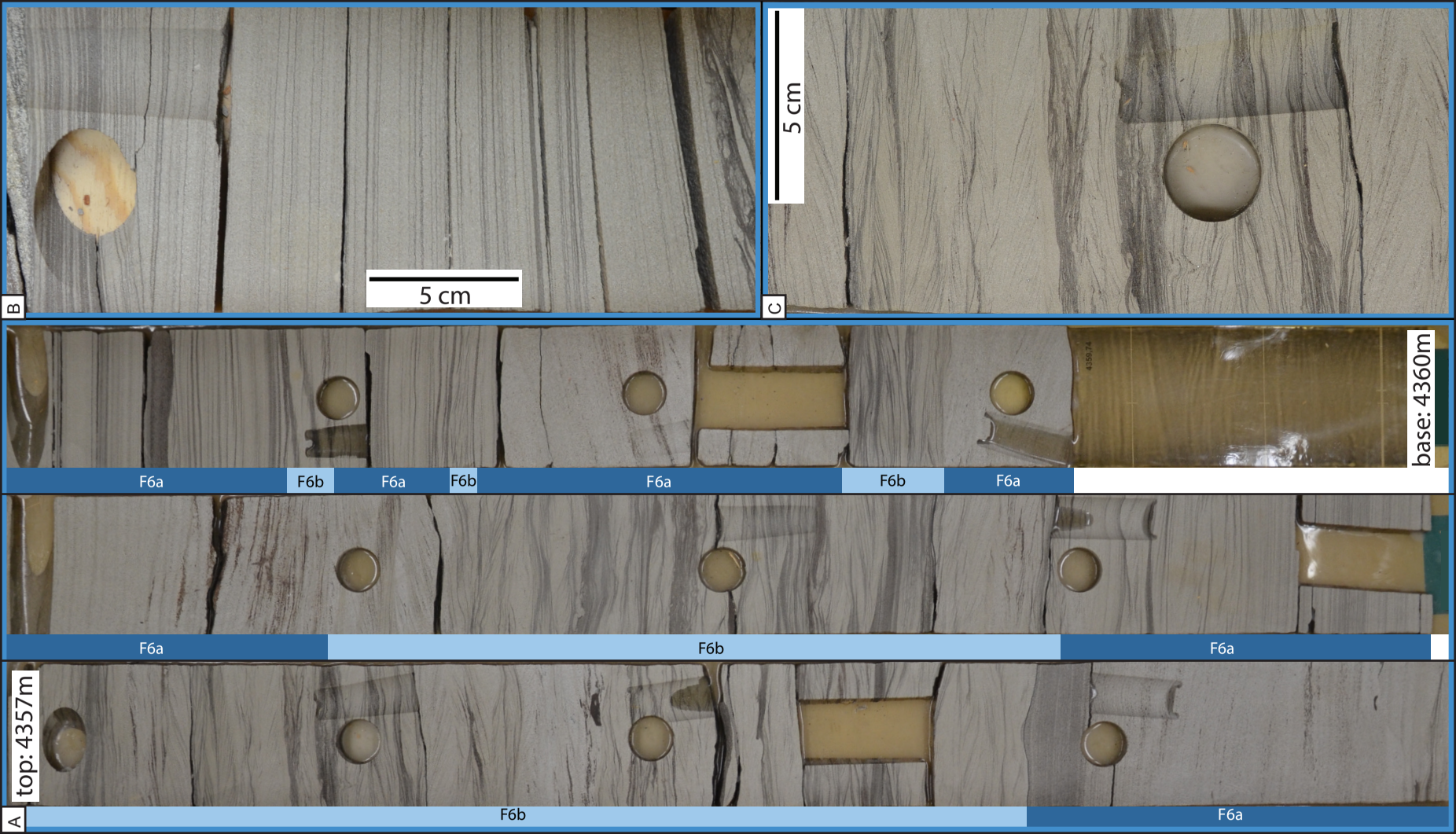
B
5 cm
C
5 cm
base: 4360m
F6a
F6b
F6a
F6b
F6a
F6b
F6a
F6a
F6b
F6a
top: 4357m
A
F6b
F6a

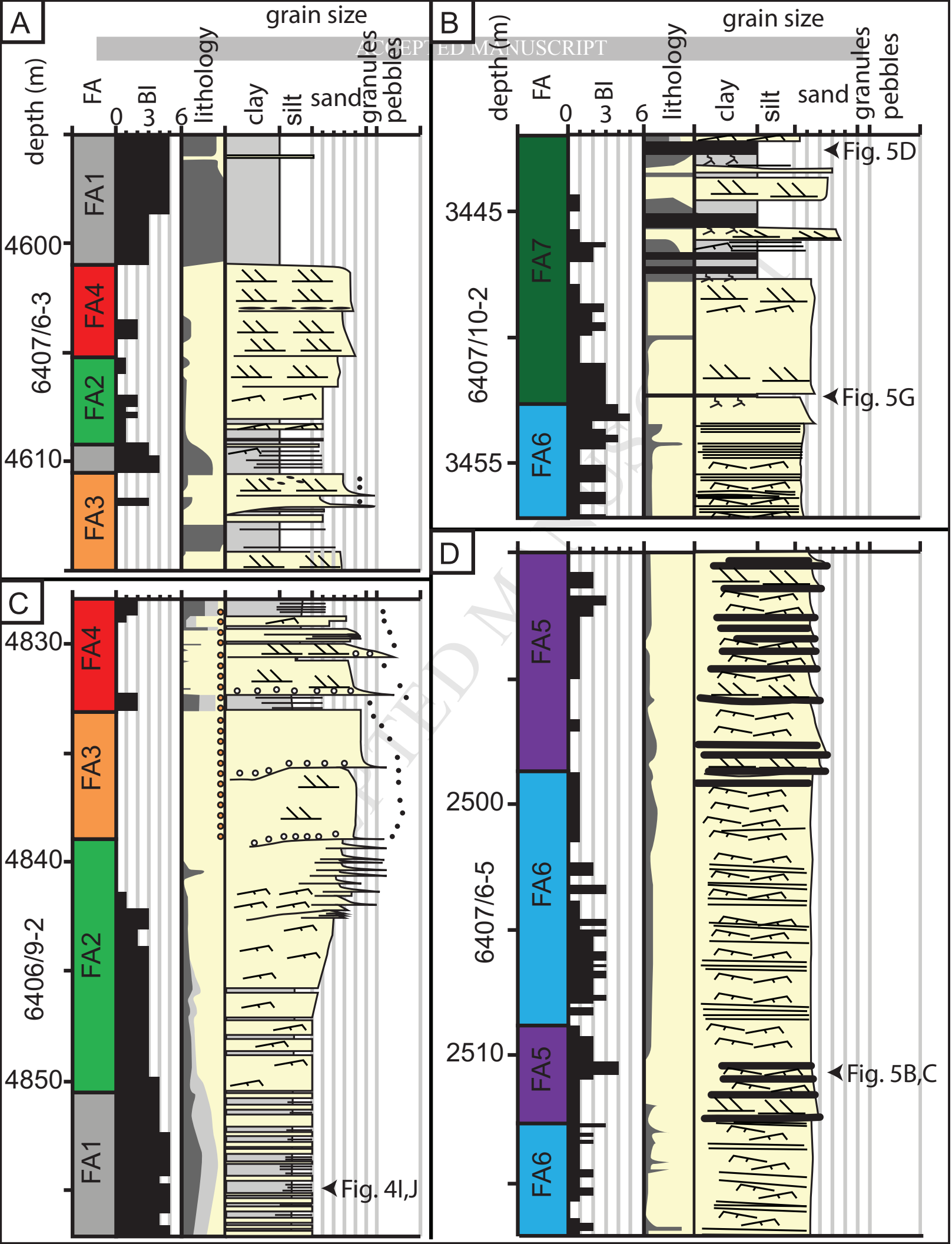

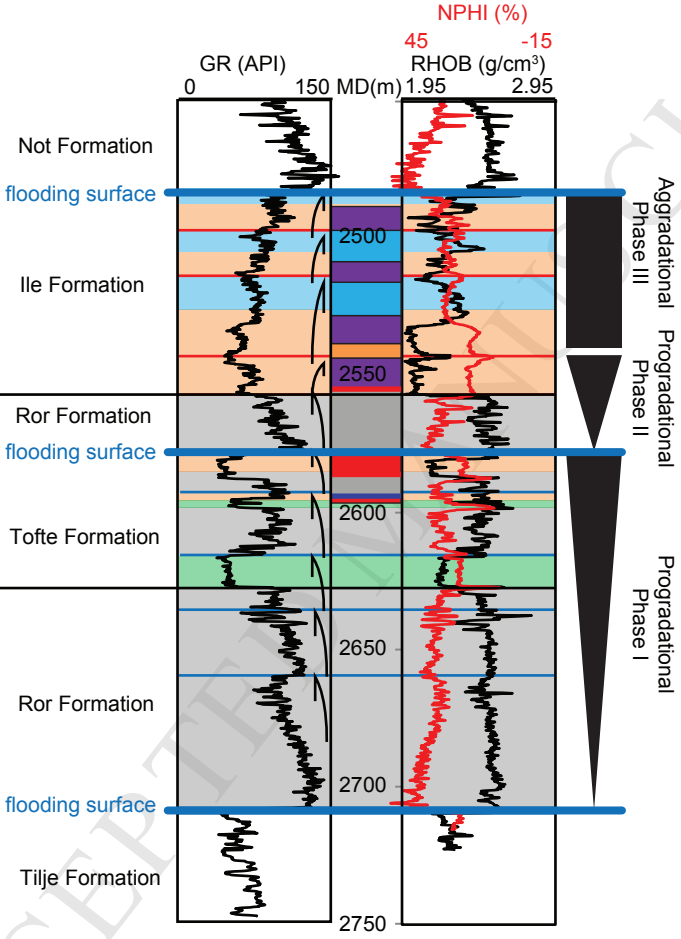


**Facies associations**

- FA6: Tidal coastline
- FA5: Tidal channel
- FA4: Marine-influenced channel
- FA3: Fluvial channel
- FA2: Delta front and mouth bar
- FA1: Prodelta and offshore

**Wireline log facies**

- HFSS: heterolithic fine grained sandstone (FA5,6)
- CSS: coarse-grained sandstone (FA3,4,5)
- DF: coarsening upward delta front (FA2)
- OS: offshore mudstones (FA1)
- CC: condensed section

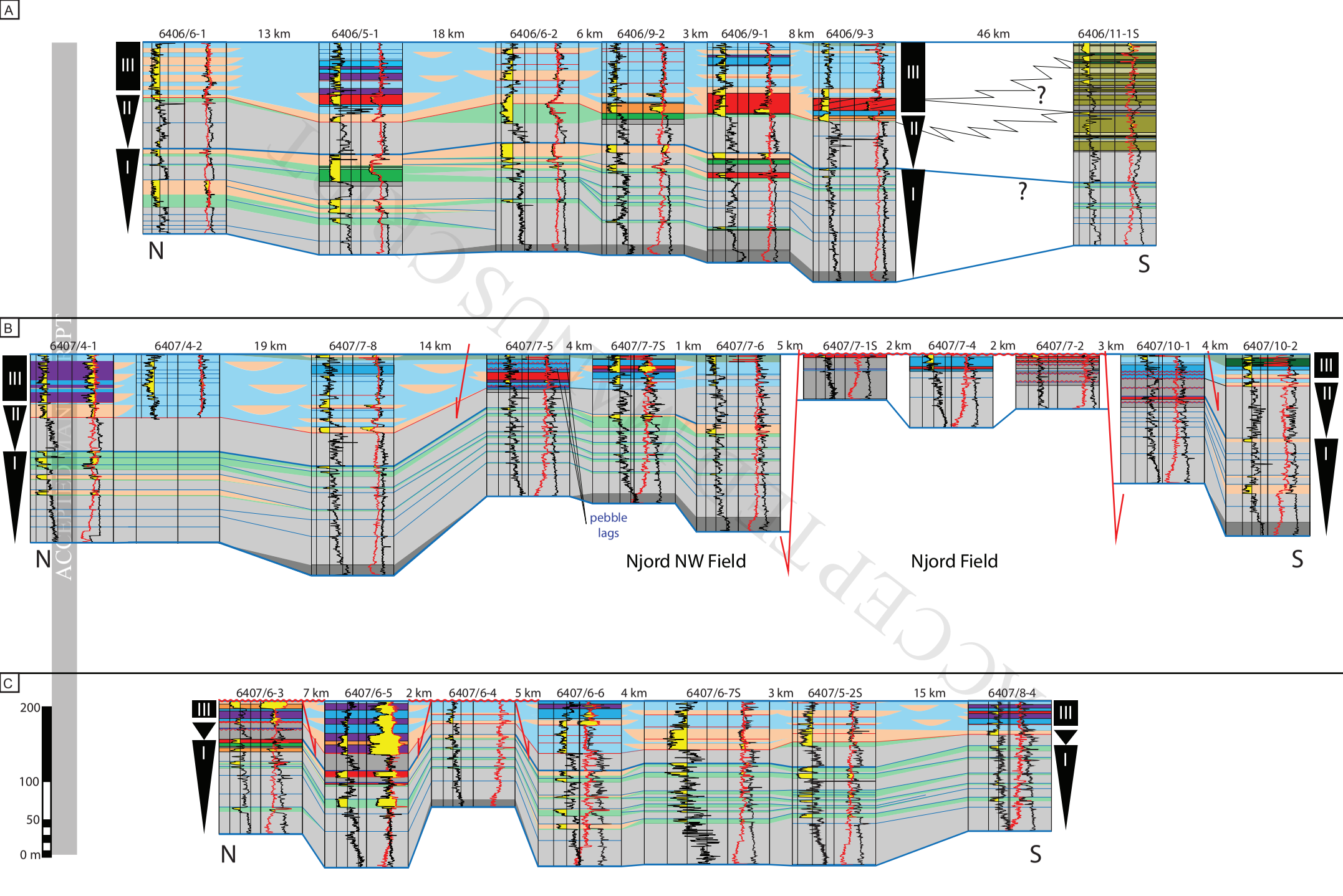
A
6406/6-1
13 km
6406/5-1
18 km
6406/6-2
6 km
6406/9-2
3 km
6406/9-1
8 km
6406/9-3
46 km
6406/11-1S
III
II
I
?
?
N
S
B
6407/4-1
6407/4-2
19 km
6407/7-8
14 km
6407/7-5
4 km
6407/7-7S
1 km
6407/7-6
5 km
6407/7-1S
2 km
6407/7-4
2 km
6407/7-2
3 km
6407/10-1
4 km
6407/10-2
III
II
I
pebble
lags
N
Njord NW Field
Njord Field
S
C
200
100
50
0 m
6407/6-3
7 km
6407/6-5
2 km
6407/6-4
5 km
6407/6-6
4 km
6407/6-7S
3 km
6407/5-2S
15 km
6407/8-4
III
I
N
S

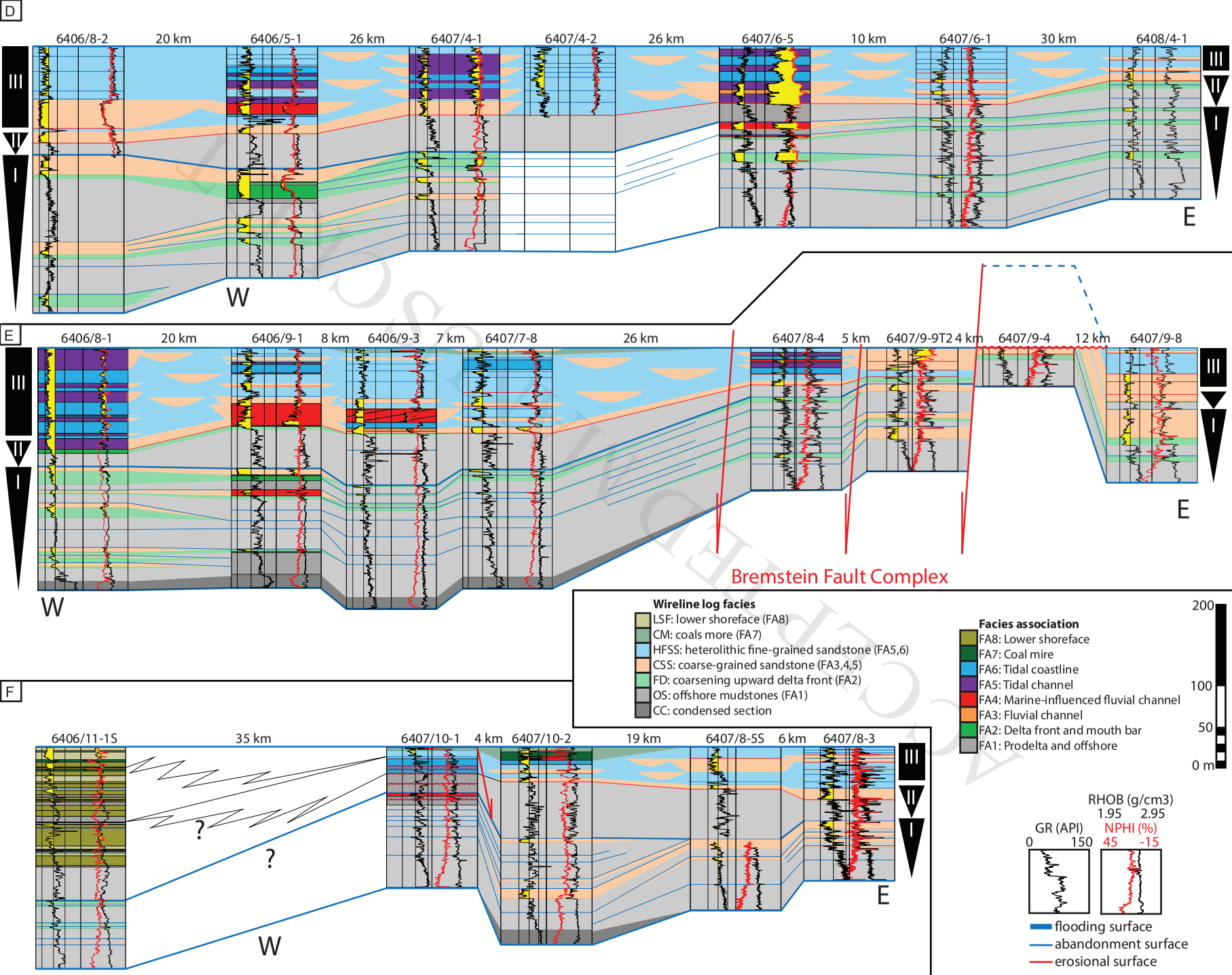
D
6406/8-2
20 km
6406/5-1
26 km
6407/4-1
6407/4-2
26 km
6407/6-5
10 km
6407/6-1
30 km
6408/4-1
III
II
I
W
E
E
6406/8-1
20 km
6406/9-1
8 km
6406/9-3
7 km
6407/7-8
26 km
6407/8-4
5 km
6407/9-9T2
4 km
6407/9-4
12 km
6407/9-8
Bremstein Fault Complex
F
6406/11-1S
35 km
6407/10-1
4 km
6407/10-2
19 km
6407/8-5S
6 km
6407/8-3
?
?
Wireline log facies
LSF: lower shoreface (FA8)
CM: coals more (FA7)
HFSS: heterolithic fine-grained sandstone (FA5,6)
CSS: coarse-grained sandstone (FA3,4,5)
FD: coarsening upward delta front (FA2)
OS: offshore mudstones (FA1)
CC: condensed section
Facies association
FA8: Lower shoreface
FA7: Coal mire
FA6: Tidal coastline
FA5: Tidal channel
FA4: Marine-influenced fluvial channel
FA3: Fluvial channel
FA2: Delta front and mouth bar
FA1: Prodelta and offshore
200
100
50
0 m
RHOB (g/cm3)
1.95
2.95
GR (API)
NPHI (%)
0
150
45
-15
flooding surface
abandonment surface
erosional surface

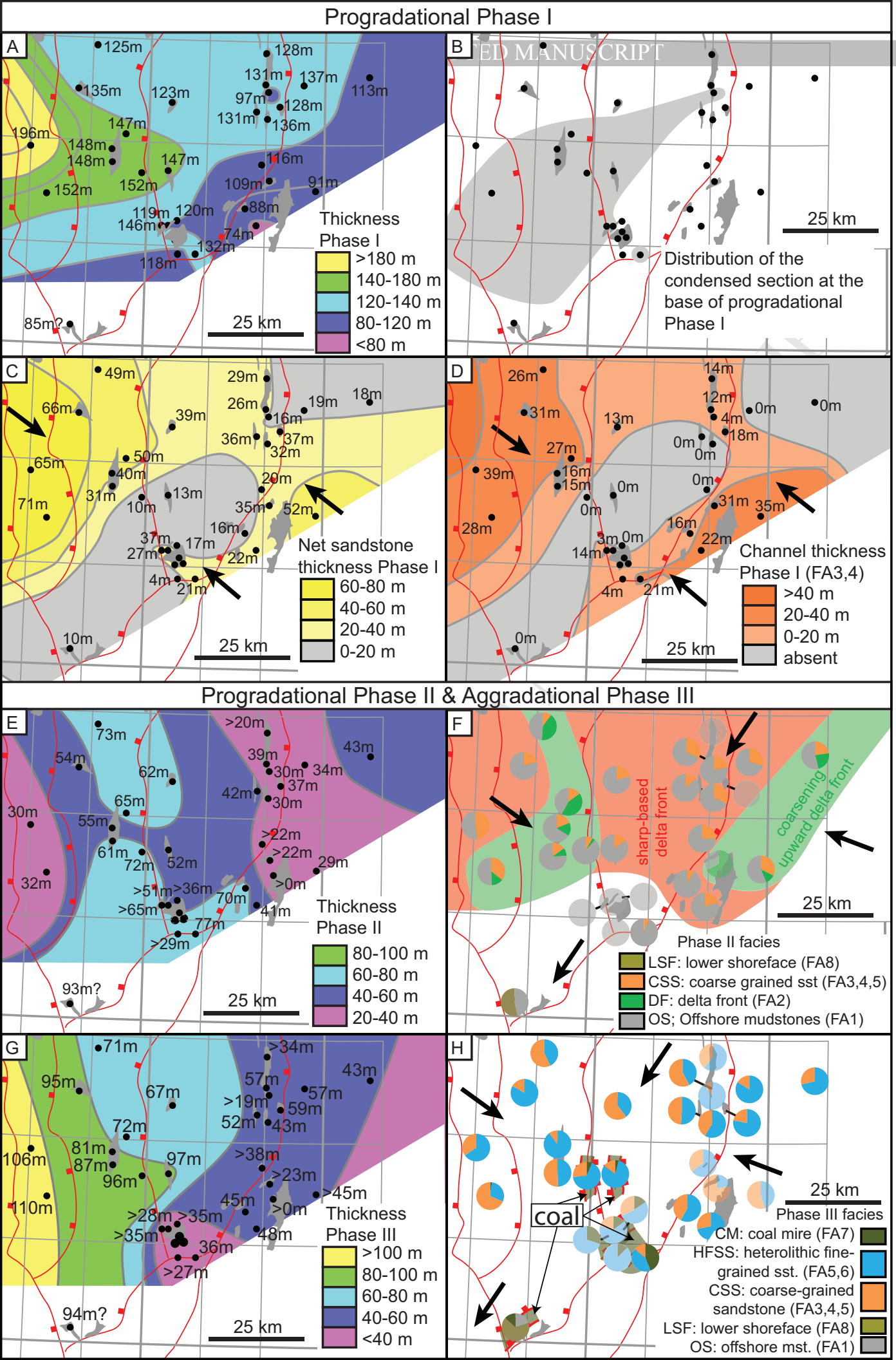

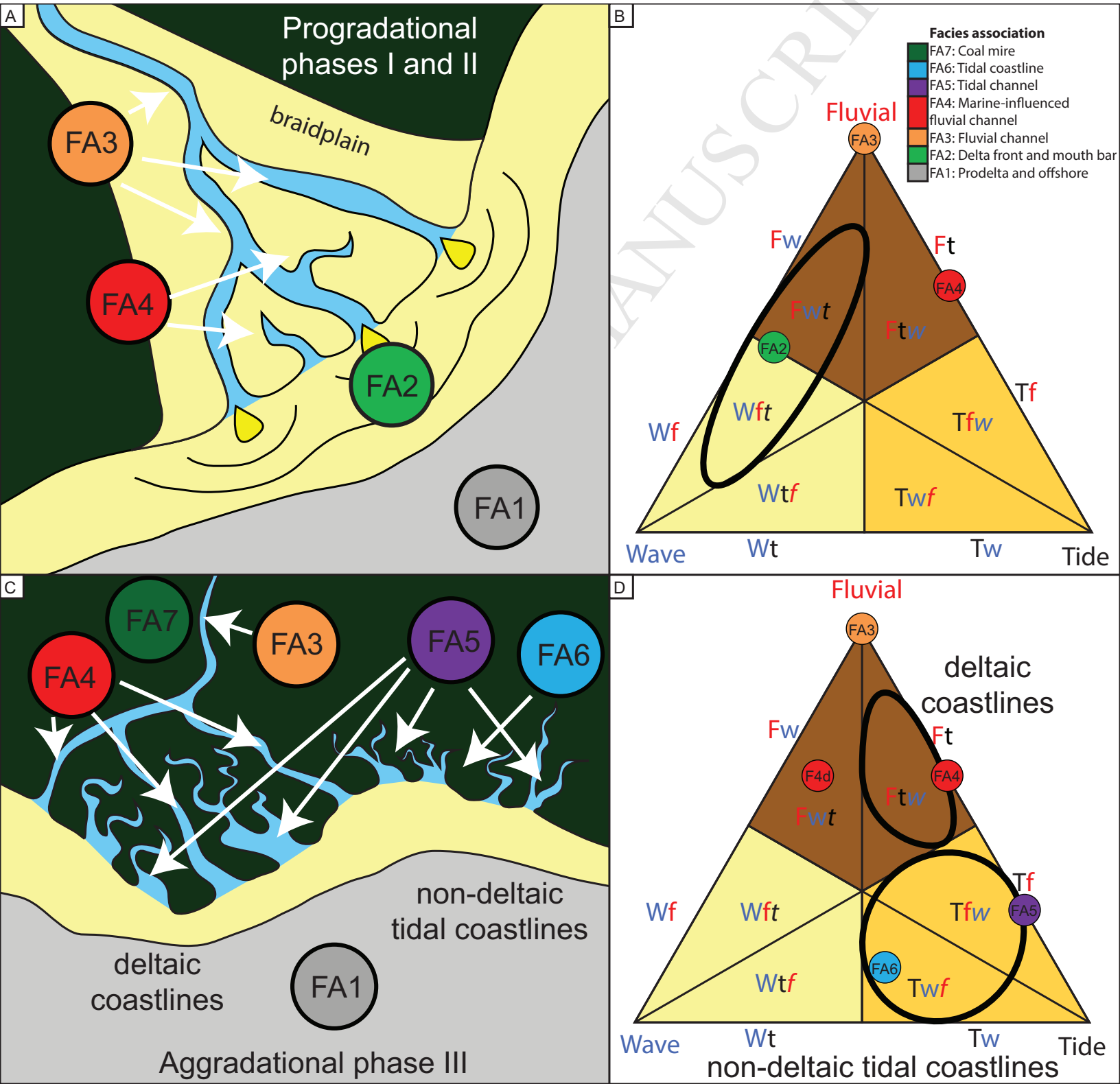
A
Progradational
phases I and II
braidplain
FA3
FA4
FA2
FA1
B
Facies association
FA7: Coal mire
FA6: Tidal coastline
FA5: Tidal channel
FA4: Marine-influenced
fluvial channel
FA3: Fluvial channel
FA2: Delta front and mouth bar
FA1: Prodelta and offshore
Fluvial
FA3
Fw
Ft
FA4
Fwt
Ftw
FA2
Tf
Wft
Tfw
Wf
Wtf
Twf
Wave
Wt
Tw
Tide
C
FA7
FA3
FA4
FA5
FA6
non-deltaic
tidal coastlines
deltaic
coastlines
FA1
Aggradational phase III
D
Fluvial
FA3
deltaic
coastlines
Fw
Ft
F4d
FA4
Ftw
Fwt
Tf
Wf
Wft
Tfw
FA5
FA6
Wtf
Twf
Wave
Wt
Tw
Tide
non-deltaic tidal coastlines